Chinese Journal of Chemical Engineering 76 (2024) 301–317

Contents lists available at ScienceDirect

Chinese Journal of Chemical Engineering

journal homepage: www.elsevier.com/locate/CJChE

Full Length Article

Optimization of capacity configuration and comprehensive evaluation of a renewable energy electrolysis of water for hydrogen production system

Huairong Zhou [1,*], Xin Wu [1], Chunlei Li [1], Siyu Yang [2], Zhichen Chen [3], Jun Lu [3], Chen Fang [3]

[1] *School of Petrochemical Engineering, Lanzhou University of Technology, Lanzhou 730050, China*
[2] *School of Chemical Engineering, South China University of Technology, Guangzhou 510640, China*
[3] *PetroChina Yumen Oilfield Company, Yumen 735200, China*

ARTICLE INFO

Article history:
Received 28 March 2024
Received in revised form
6 September 2024
Accepted 8 September 2024
Available online 30 September 2024

Keywords:
Renewable energy
Green hydrogen production
Multi-energy coupling
Capacity optimization
System optimization

ABSTRACT

The global green hydrogen industry is experiencing rapid growth, but the high production costs are hindering its widespread adoption. To address this challenge, it is particularly important to rationally configure a renewable energy hydrogen production system. For this purpose, the study proposes a model for capacity optimization configuration of a renewable energy hydrogen production system, which integrates wind power, photovoltaic (PV) power, and concentrating solar power (CSP) with alkaline electrolyzer. It conducts capacity optimization configuration and comprehensive evaluations of the hydrogen production system across various scenarios. To minimize the total daily consumption cost, the CPLEX solver is utilized to solve the objective function and determine the capacity configuration of the renewable energy electrolysis of water hydrogen production system generator set under various scenarios. This approach achieves a utilization rate of over 99% for renewable energy. Through comprehensive evaluation, research has found that renewable energy-coupled hydrogen production significantly reduces generator capacity and electricity generation costs compared to separate hydrogen production, enhancing the economic efficiency of the system. The Wind-PV-CSP coupling hydrogen production system has the smallest generator assembly capacity and the lowest hydrogen production cost, which is 18.84 $CNY \cdot kg^{-1}$, significantly lower than the cost of PV-CSP coupling hydrogen production (25.78 $CNY \cdot kg^{-1}$) and wind-PV coupling hydrogen production (25.86 $CNY \cdot kg^{-1}$). It has good development prospects and plays an important role in exploring the development path of large-scale on-site consumption of new energy.

1. Introduction

Hydrogen energy is a form of secondary energy derived from abundant sources, environmentally friendly, and low in carbon emissions [1]. It is primarily utilized in the energy, chemical industry, transportation, metallurgy, and other sectors [2]. Hydrogen energy will play an important role in solving the global energy crisis, climate warming, and other issues [3]. It will also become a strategic choice for China to build a new energy system and achieve the goal of dual carbon. As the world's largest hydrogen producer, China mainly produces hydrogen from fossil fuels. However, this production process generates a significant amount of CO_2, which does not align with the requirements for clean and low-carbon production [4]. With the deepening revolution in energy production and consumption, the government has increasingly focused on the proportion of green hydrogen in hydrogen production [5]. In March 2022, the Chinese government issued the "Medium and Long-Term Plan for the Development of the Hydrogen Energy Industry (2021–2035)", which clearly outlines that the widespread adoption of green hydrogen will be accomplished by 2030. The development of the green hydrogen industry can not only replace hydrogen production from fossil energy sources but also promote

* Corresponding author.
E-mail address: zhouhr@lut.edu.cn (H. Zhou).

https://doi.org/10.1016/j.cjche.2024.09.003
1004-9541/

the large-scale local consumption of renewable energy and accelerate the transformation of the energy system [6].

Green hydrogen refers to the use of renewable energy sources such as wind energy, solar energy, hydraulic energy, nuclear energy, and biomass energy to electrolyze water and produce hydrogen, as illustrated in Fig. 1. China has become the world's largest in installed capacity of renewable energy. Its wind and solar power generation ranks first globally. The rapid development of renewable energy has brought new challenges to the power system, the most prominent of which is the high proportion of wind and solar energy curtailment and local consumption issues. These challenges are mainly caused by the fluctuation of the output power of wind farms and photovoltaic fields. With the continuous development of the power system, the advantages of green hydrogen technology in promoting the consumption of renewable energy are becoming increasingly prominent [7]. In recent years, several green hydrogen projects have been initiated, approved, or commenced construction in China. For example, China's first wind power hydrogen production project, the "Hebei Jiantou Wind Power Hydrogen Production Project," utilizes a 200 MW capacity wind farm for electricity generation to power a 10 MW scale electrolyzer system. The project has successfully produced over 600 tons of hydrogen after a trial operation. The "China Huadian 200000 kW New Energy Hydrogen Production Demonstration Project" is China's first large-scale renewable energy hydrogen production demonstration project. It utilizes 120000 kW of wind power, 80000 kW of photovoltaic power, and 20000 kW of electrochemical energy storage to produce hydrogen through the electrolysis of water. The project has an annual output of 7800 tons of green hydrogen. Duolun County's "Datang Duolun 150000-kW Wind Hydrogen Production Integration Technology Demonstration Project" aims to produce 5419 tons of hydrogen per year. According to relevant statistics, the scale of green hydrogen projects implemented in China has reached 49000 tons, and the total capacity of approved green hydrogen projects is about 2.7 million tons [8]. Hydrogen production through electrolytic water technology can not only enhance the utilization rate of renewable energy but also enable on-site consumption of renewable energy [9].

At present, there are still some challenges in the large-scale production of the green hydrogen industry. Scholars have conducted relevant studies on wind power hydrogen production and photovoltaic hydrogen production. Zhang *et al.* [10] established an economic cost model for the hydrogen production system of wind power. Based on the data related to the investigated wind energy resources, the optimal capacity configuration of the electrolyzer, hydrogen storage tank, and wind power generation device in the system, as well as the optimal scheduling scheme of the system, were determined with the hydrogen production cost as the target. By comparing the data from various regions, it is concluded that the most significant factors influencing the cost of hydrogen production are the investment cost of equipment and the efficiency of the electrolyzer. Zhang *et al.* [11] analyzed the life cycle of hydrogen production systems for onshore and offshore wind power, taking into account environmental factors. The results indicated that hydrogen production from onshore wind power was more efficient compared to hydrogen production from offshore wind power. Shin *et al.* [12] studied the economics of hydrogen production through electrolysis of water using renewable energy in various scenarios. They determined the energy consumption for hydrogen production by analyzing output data from various renewable energy sources and the efficiency data of different electrolyzer systems. According

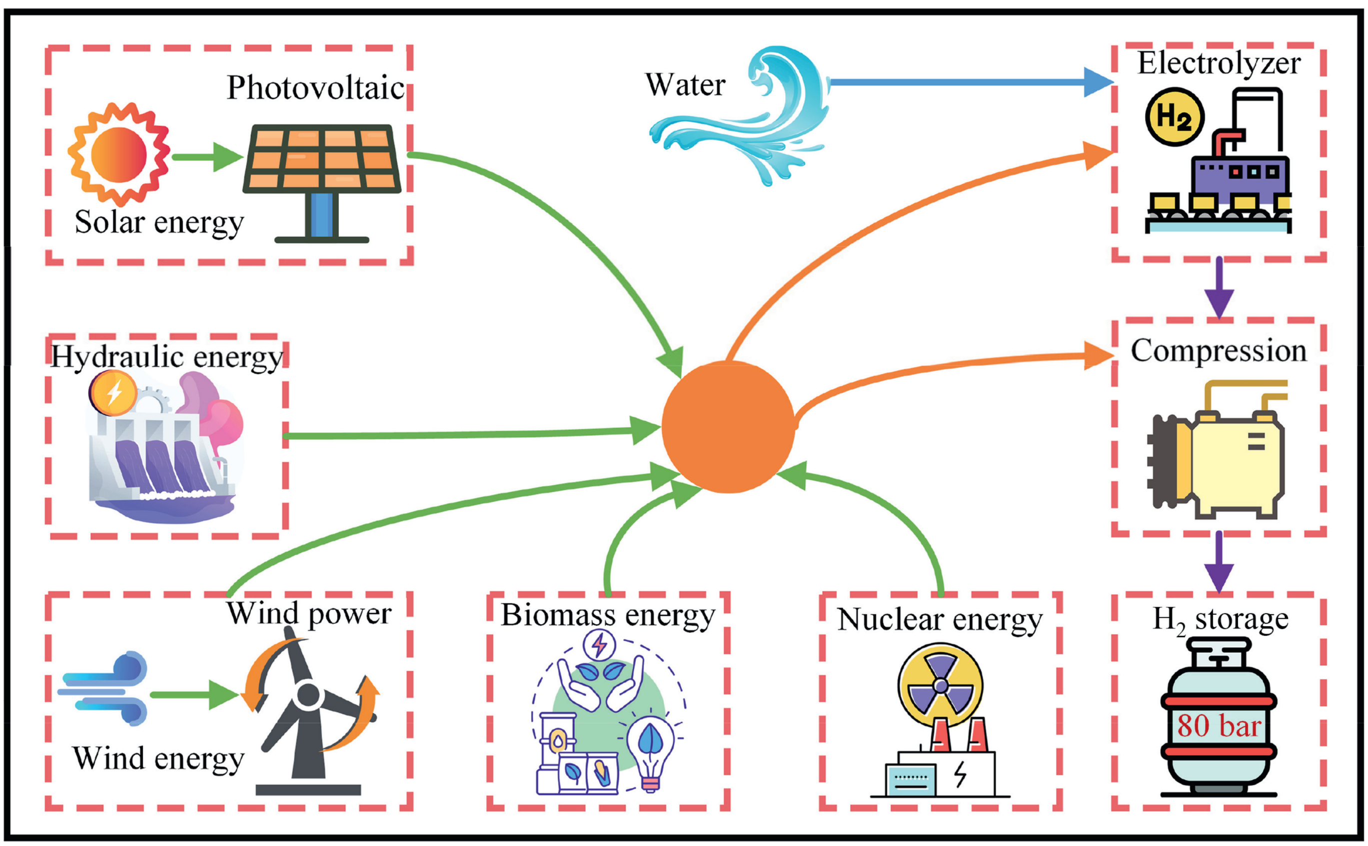

Fig. 1. Schematic diagram of green hydrogen production.

to the efficiency and cost of hydrogen production, the levelized cost of hydrogen production is calculated under various conditions. The results indicate that the most effective method for hydrogen production involves onshore wind power and an alkaline electrolyzer. Li *et al.* [13] proposed a model for combined power generation that integrates photovoltaic (PV) hydrogen production and hydrogen fuel cells. After simulation and calculation using Simulink, the study found that the implementation of hydrogen energy storage enhanced the utilization of renewable energy in the system.

The aforementioned research has yielded results in wind power hydrogen production and photovoltaic hydrogen production. However, the renewable energy system in the hydrogen production setup is inadequate, leading to high production costs for hydrogen. Han *et al.* [14] studied the system capacity and logistics scheduling under the minimum power generation cost of the electricity-hydrogen-methanol-electricity system. They proved that the wind-PV coupled power generation hydrogen production system is superior to independent wind power or photovoltaic hydrogen production. Ibanez-Rioja *et al.* [15] studied a green hydrogen production system that integrates photovoltaic and wind power, batteries, and an alkaline electrolyzer. Aiming to minimize the levelized cost of hydrogen production, researchers utilized an evolutionary algorithm to optimize the objective function, achieved the capacity optimization configuration of components and system control strategy, and analyzed the future cost of hydrogen production. The feasibility of the wind-PV coupled hydrogen production system has been demonstrated. Shi *et al.* [16] proposed a wind-solar complementary coupled hydrogen production system. They used spectrum analysis to calculate and analyze the output of wind power and photovoltaic energy across various time scales. The study demonstrated the complementary relationship between wind power and photovoltaic output, providing a theoretical basis for large-scale green hydrogen production. Ren *et al.* [17] developed a hybrid hydrogen production system that integrates wind power and photovoltaic power. The system includes a pumped energy storage device and aims to address the issues of volatility and high abandonment rates of wind and photovoltaic power after integration into the grid. By utilizing simulation software, the wind power output and photovoltaic power output models were comprehensively analyzed, resulting in the derivation of the complementary characteristic curve of wind power and photovoltaic power. The study found that the wind-solar complementary system could not fully meet the electricity demand of the system. The integration of a pumped energy storage system helped stabilize the fluctuations of wind and solar power. The system's capacity is optimized using the particle swarm optimization algorithm. This process determines the capacity of the electrolytic cell, battery, and energy storage equipment for storing energy, thereby enhancing the system's ability to absorb wind and electricity. Phan-Van *et al.* [18] proposed a comprehensive feasibility evaluation model for offshore wind power photovoltaic coupled hydrogen production. They calculated related parameters, such as the capacity of the renewable energy hydrogen production system and the cost of hydrogen production. In addition, a model for configuring the capacity of an electrolyzer is constructed to determine the optimal capacity configuration through analysis and comparison, resulting in reduced production costs.

Numerous studies have demonstrated that combining wind power with photovoltaic technology for hydrogen production is more effective than relying solely on wind power or photovoltaic systems for hydrogen production. Renewable energy power generation systems need to be adjusted before they can be used in electrolyzers. The fluctuation in wind power and photovoltaic output causes disruptions in the smooth operation of the hydrogen production system. Many researchers depend on the power grid or thermal power generation to maintain the electric balance of the hydrogen production system, leading to a significant amount of CO_2 emissions. To explore clean and low-carbon hydrogen production methods, concentrating solar power has become the focus of attention. China's concentrating solar power generation is rapidly emerging, and the installed capacity in 2021 has reached 590 MW. Concentrating solar power generation has the advantages of being low carbon, clean, having energy storage capabilities, and possessing strong adjustment capabilities. Some researchers have considered incorporating concentrating solar power stations into renewable energy hydrogen production systems to reduce CO_2 emissions. Yang *et al.* [19] proposed a comprehensive energy hydrogen production system that includes a concentrating solar power station. By setting the maximum net income of the system as the objective function, the system was solved using the CPLEX solver. This process helped determine the optimal capacity configuration of the hydrogen storage tank and concentrating solar power station, ultimately enhancing the system's economic efficiency. The results show that the concentrating solar power station not only greatly reduces CO_2 emissions but also significantly improves the utilization rate of solar energy. Zhang *et al.* [20] investigated the feasibility and economic aspects of integrating concentrating solar power into a photovoltaic hydrogen production system. Through calculation and analysis, they demonstrated that a PV-CSP coupled hydrogen production system was superior to photovoltaic hydrogen production. Therefore, concentrating solar power will play an important role in the research of hydrogen production systems that utilize electrolysis of water from renewable energy sources.

Based on existing studies and reports, it has been found that the cost of hydrogen production is the primary factor influencing the large-scale production of renewable energy electrolytic water hydrogen production systems. Current research primarily focuses on wind power, photovoltaic systems, and hydrogen production, with limited attention given to the utilization of concentrating solar power stations in renewable energy generation. Existing studies primarily focus on optimizing the capacity allocation of electrolyzer sizes. However, there is a lack of in-depth research on the capacity allocation of renewable energy sources. Therefore, it is crucial to allocate the capacity of the generator set rationally in the renewable energy hydrogen production system to reduce the cost of hydrogen production.

In the future, wind power, photovoltaic power, and concentrating solar power will combine to form a multi-energy complementary renewable energy generation system for producing hydrogen. This integration is expected to become an inevitable trend. Based on the hydrogen production system of renewable energy multi-energy complementary power generation, this paper first investigated wind speed resource data, solar resource data, and electrolyzer characteristics data of a region in northern China. It then established models for wind power output, photovoltaic output, battery charging, and discharging, concentrating solar power station output, and the electrolyzer. Secondly, the constraints of the relevant mathematical model were refined, and the programming calculations were conducted for hydrogen production using wind power, photovoltaic hydrogen production, concentrating solar power hydrogen production, PV-CSP coupling hydrogen production, wind-PV coupling hydrogen production, and wind-PV-CSP coupling hydrogen production. The CPLEX solver was invoked using the YALMIP platform in MATLAB to solve the designed system for renewable energy electrolytic water hydrogen production. The optimum capacity configuration of each hydrogen production system is determined. Finally, the parameters of equipment investment cost, equipment operation and maintenance cost, oxygen income, and hydrogen production cost of a renewable energy hydrogen production system under multiple scenarios are comprehensively evaluated to determine the optimal hydrogen production scheme. Theoretical basis and calculation methods are provided for researching hydrogen production systems from electrolyzed water using renewable energy in the future. The research idea is depicted in Fig. 2.

2. Operating Framework of a Renewable Energy Electrolysis of Water Hydrogen Production System

The renewable energy electrolytic water hydrogen production system described in this paper consists of wind power generation, photovoltaic power generation, battery energy storage, a thermal collector mirror field at the concentrating solar power station, a thermal storage tank at the concentrating solar power station, turbine power generation at the concentrating solar power station, an electrolyzer, and other units. To ensure the safe and stable operation of the electrolytic cell in the system, electricity purchased from the grid is utilized to make electrical balance adjustments for renewable energy, as illustrated in Fig. 3. Using the flexibility of the programming software, the capacity configuration of the generator set, and the hydrogen production cost of the system in the renewable energy electrolytic water hydrogen production system were calculated under different scenarios. The operational characteristics of each scenario were analyzed based on the calculation results, and the

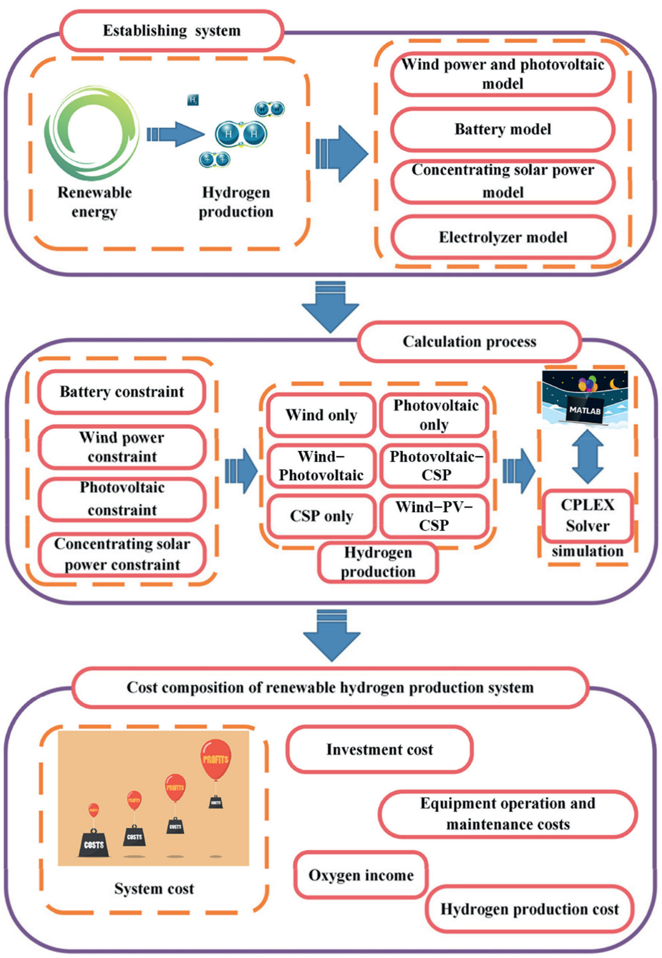

Fig. 2. Research idea: capacity optimization allocation of renewable energy for electrolytic water hydrogen production system.

study explored the renewable energy electrolytic water hydrogen production scheme with better development prospects.

2.1. Output model of wind power generation system

The output power of wind power generation is mainly determined by wind speed, and it is expressed as follows [21]:

$$P_{\text{wind}}^{\text{O}}(t)=\begin{cases}0 & v(t)\le v^{\text{I}},v(t)\ge v^{\text{O}}\\ \gamma\cdot P_{\text{wind}}^{\text{R}} & v^{\text{I}}<v(t)<v^{\text{R}}\\ P_{\text{wind}}^{\text{R}} & v^{\text{R}}\le v(t)\le v^{\text{O}}\end{cases} \tag{1}$$

$$\gamma=\frac{[v(t)]^3-(v^{\text{I}})^3}{(v^{\text{R}})^3-(v^{\text{I}})^3} \tag{2}$$

The above equation, $P_{\text{wind}}^{\text{O}}(t)$ is the output power of the wind farm at time t, kW. $P_{\text{wind}}^{\text{R}}$ is the rated power of a wind turbine in a wind farm, kW. $v(t)$ is the wind speed at time t, m·s^{-1}. v^{I}, v^{O}, v^{R} respectively, it refers to the cut-in wind speed, cut-out wind speed, and rated wind speed, m·s^{-1}.

2.2. Photovoltaic power output model

The output power of photovoltaic power generation is mainly determined by the light intensity, and this relationship can be expressed as [22]:

$$P_{\text{pv}}^{\text{O}}(t)=[1+\kappa\cdot(T-25)]\cdot P_{\text{pv}}^{\text{R}}\cdot\frac{\Gamma}{\Gamma_{\text{n}}} \tag{3}$$

The above equation, $P_{\text{pv}}^{\text{O}}(t)$ is the output power of a photovoltaic power station at time t, kW; P_{pv}^{R} is the rated power of a photovoltaic power station, kW. κ is the temperature coefficient of solar cell panel power is measured in percentage, %; T is the actual operating temperature of the solar cell panel, °C; Γ is the actual amount of radiation absorbed by the solar panel, W·m^{-2}.

2.3. Battery model

Hydrogen production systems that rely on wind power or photovoltaic renewable energy sources need to incorporate a battery energy storage system. An electric energy storage system can enhance the utilization of wind and photovoltaic power, as well as ensure the stable production of hydrogen in renewable energy systems. Therefore, the inclusion of a battery energy storage model plays a crucial role in the green hydrogen model developed by this research [23].

The simple mathematical expression of the battery model is [24]:

$$P_{\text{sb}}^{\text{S}}(t)=\left(1-\eta_{\text{sb}}^{\text{L}}\right)\cdot P_{\text{sb}}^{\text{S}}(t-1)\cdot\left[\eta_{\text{ch}}\cdot P_{\text{sb}}^{\text{CH}}(t)-\left(\frac{P_{\text{sb}}^{\text{DISCH}}(t)}{\eta_{\text{disch}}}\right)\right]\cdot\Delta t \tag{4}$$

The above equation, $P_{\text{sb}}^{\text{S}}(t)$ is the electric power stored in the battery at time t, kW. $\eta_{\text{sb}}^{\text{L}}(t)$ is the loss rate of the battery at time t. η_{ch}, η_{disch} respectively, the charging and discharging efficiency of the battery $P_{\text{sb}}^{\text{CH}}(t)$, $P_{\text{sb}}^{\text{DISCH}}(t)$ is the charge and discharge power of the battery at time t, kW.

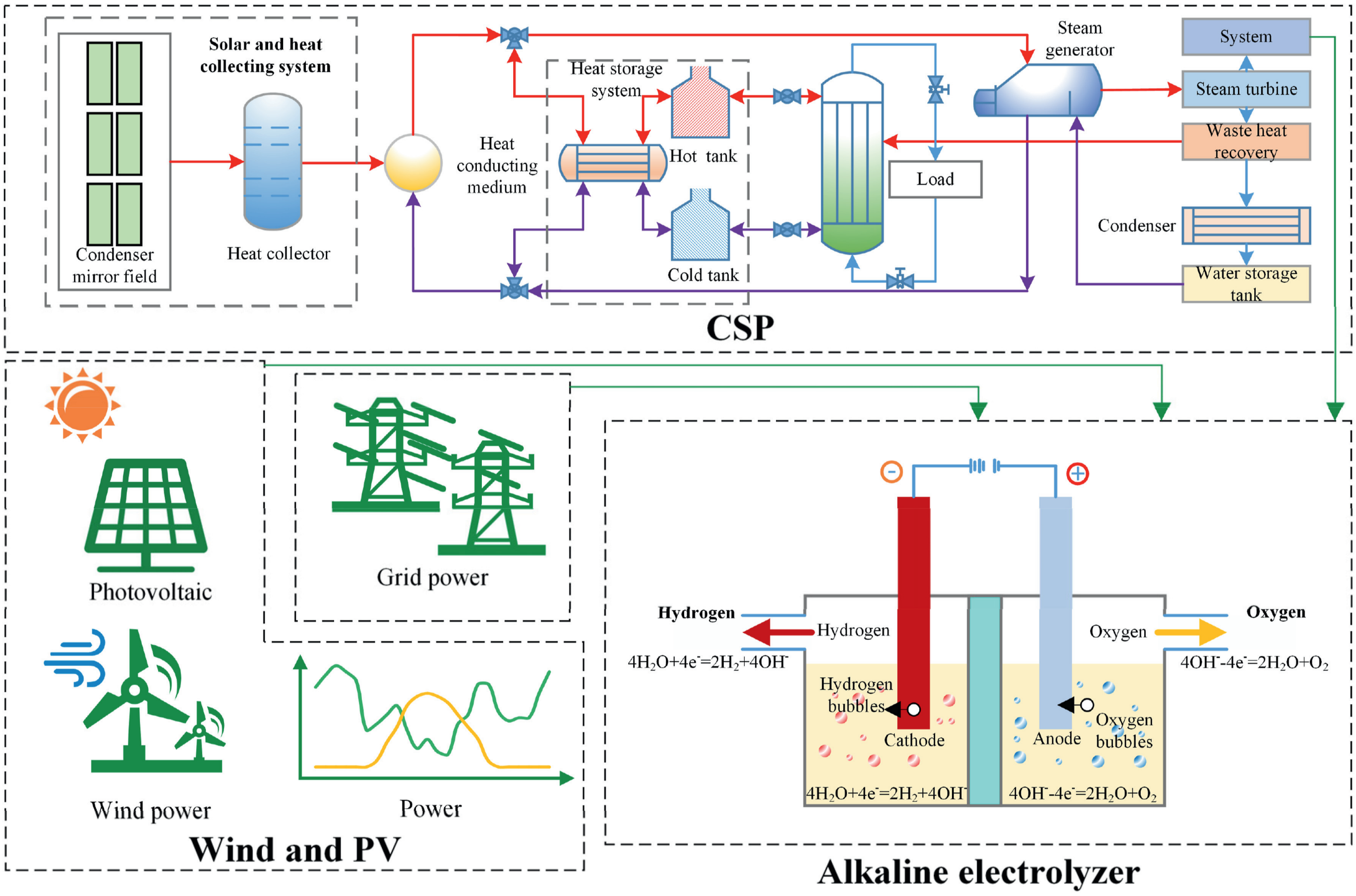

Fig. 3. Flow chart depicting the operational framework of a hydrogen production system from electrolyzed water using renewable energy.

2.4. Output power model of a concentrating solar power station

A concentrating solar power station is mainly composed of three parts: a light-gathering heat collection system, a heat storage system, and a steam turbine power generation system [25]. The model is expressed as follows [26]:

$$P_{\mathrm{csp}}^{\mathrm{G}}(t)=(1-\eta_{\mathrm{hl}})\cdot\left(\eta_{\mathrm{cs}}\cdot S_{\mathrm{mf}}\cdot D(t)\right) \tag{5}$$

$$P_{\mathrm{csp}}^{\mathrm{G}}(t)-P_{\mathrm{csp}}^{\mathrm{U}}(t)-P_{\mathrm{tur}}^{\mathrm{IN}}(t)-P_{\mathrm{hs}}^{\mathrm{IN}}(t)+P_{\mathrm{hs}}^{\mathrm{OUT}}(t)=0 \tag{6}$$

$$P_{\mathrm{tur}}^{\mathrm{IN}}(t)=P_{\mathrm{tur}}^{\mathrm{STA}}(t)+P_{\mathrm{tur}}^{\mathrm{CON}}(t) \tag{7}$$

$$P_{\mathrm{csp}}^{\mathrm{O}}(t)=\eta_{\mathrm{tc}}\cdot P_{\mathrm{tur}}^{\mathrm{IN}}(t) \tag{8}$$

$$P_{\mathrm{hs}}^{\mathrm{S}}(t)=(1-\eta_{\mathrm{hs}})\cdot P_{\mathrm{hs}}^{\mathrm{S}}(t-1)+\left[\eta_{\mathrm{hs}}^{\mathrm{IN}}\cdot P_{\mathrm{hs}}^{\mathrm{IN}}(t)-\left(\frac{P_{\mathrm{hs}}^{\mathrm{OUT}}(t)}{\eta_{\mathrm{hs}}^{\mathrm{OUT}}}\right)\right]\cdot\Delta t \tag{9}$$

The above equation, $P_{\mathrm{csp}}^{\mathrm{G}}(t)$ is the concentrating solar power collected at time t by the photothermal power station, kW. η_{hl}, η_{cs} is the efficiency of heat loss and the conversion of light intensity into heat energy during heat transfer. S_{mf} is the area of the heat-collecting mirror field is measured, m^2. $D(t)$ is the direct sunlight intensity at time t, $\mathrm{W\cdot m^{-2}}$. $P_{\mathrm{csp}}^{\mathrm{U}}(t)$, $P_{\mathrm{tur}}^{\mathrm{IN}}(t)$, $P_{\mathrm{hs}}^{\mathrm{IN}}(t)$, $P_{\mathrm{hs}}^{\mathrm{OUT}}(t)$ respectively represent the unused thermal power at time t of the concentrating solar power station, the input power at time t of the steam turbine, and the input and output power at time t of the heat storage system, kW. $P_{\mathrm{tur}}^{\mathrm{STA}}$, $P_{\mathrm{tur}}^{\mathrm{CON}}(t)$ represent the start power and power consumption of the turbine at time t, kW. $P_{\mathrm{csp}}^{\mathrm{O}}(t)$ is the output power of the concentrating solar power station at time t, kW. η_{tc} is the efficiency of converting heat into electricity. $P_{\mathrm{hs}}^{\mathrm{S}}(t)$ is the thermal power stored at time t of the thermal storage system, kW. η_{hs} refers to the efficiency of heat loss during the heat storage system's storage process. $\eta_{\mathrm{hs}}^{\mathrm{IN}}$, $\eta_{\mathrm{hs}}^{\mathrm{OUT}}$ are respectively the thermal efficiency of the heat input and output of the heat storage system.

2.5. Electrolyzer model

In this paper, a relatively mature alkaline electrolyzer is used as the research subject, and its input power is:

$$P_{\mathrm{ele}}^{\mathrm{W}}(t)=P_{\mathrm{wind}}^{\mathrm{O}}(t)+P_{\mathrm{pv}}^{\mathrm{O}}(t)+P_{\mathrm{csp}}^{\mathrm{O}}(t)+P_{\mathrm{grid}}^{\mathrm{BUG}}(t) \tag{10}$$

The above equation, $P_{\mathrm{ele}}^{\mathrm{W}}(t)$ is the working power of the electrolyzer at time t, kW. $P_{\mathrm{grid}}^{\mathrm{BUG}}(t)$ is the power purchased by the system at time t, kW.

The relationship between hydrogen output and input power in an electrolyzer can be determined from the Ref. [27]. 1 kW of electricity can produce 9.33 mol of hydrogen. The relationship between hydrogen and electricity can be expressed as:

$$Y_{\mathrm{ele}}^{\mathrm{H_2}}(t)=\delta^{\mathrm{H_2}}\cdot P_{\mathrm{ele}}^{\mathrm{W}}(t) \tag{11}$$

The above equation, $Y_{ele}^{H_2}(t)$ is the hydrogen production at time t of the electrolyzer, mol. δ^{H_2} is 9.33 $mol\cdot kW^{-1}$.

When the electrolytic water hydrogen production system generates an excess of hydrogen, the surplus hydrogen must be stored in the tank. The hydrogen balance is:

$$D^{H_2}(t)+V^{H_2}(t)=Y_{ele}^{H_2}(t) \tag{12}$$

The above equation, $D^{H_2}(t)$ is the quantity of hydrogen demanded at time t. $V^{H_2}(t)$ represents the quantity of hydrogen in the tank at time t, mol.

According to the stoichiometric relationship of hydrogen production from electrolytic water, it can be seen that hydrogen production is twice that of oxygen production. Therefore, the oxygen production is:

$$Y_{ele}^{O_2}(t)=0.5\times Y_{ele}^{H_2}(t) \tag{13}$$

The above equation, $Y_{ele}^{O_2}(t)$ is the amount of oxygen produced by the electrolyzer at time t in the mole.

3. Capacity Optimization of the Generator Set in the System

The greater the capacity of wind, photovoltaic, and concentrating solar power stations in a renewable energy electrolytic water hydrogen production system, the lower the electricity purchased from the grid. However, the cost of the system investment will also rise. The key issue addressed in this paper is how to allocate the installed capacity of wind, photovoltaic, and concentrating solar power stations to ensure the lowest hydrogen production cost while reducing power purchase from the grid.

3.1. Construction of a capacity optimization allocation model

This paper optimizes the system intending to minimize the total daily consumption cost. The total system cost includes equipment investment cost, equipment operation and maintenance cost, and oxygen income cost. Therefore, the expression of the objective function is as follows:

$$C_{total}=\min\sum\left(C_{inv}+C_{run}+C_{pur}-C_{inc}\right) \tag{14}$$

$$C_{inv}=P_{wind}\cdot C_{wind}^{INV}+P_{pv}\cdot C_{pv}^{INV}+P_{csp}\cdot C_{csp}^{INV}+P_{ele}\cdot C_{ele}^{INV}+M^{H_2}C_{st}^{INV} \tag{15}$$

$$C_{run}=C_{wind}^{RUN}+C_{pv}^{RUN}+C_{csp}^{RUN}+C_{ele}^{RUN} \tag{16}$$

$$C_{wind}^{RUN}=\sum_{t=1}^{24}\left(\xi_{wind}\cdot P_{wind}^{O}(t)\right) \tag{17}$$

$$C_{pv}^{RUN}=\sum_{t=1}^{24}\left(\xi_{pv}\cdot P_{pv}^{O}(t)\right) \tag{18}$$

$$C_{csp}^{RUN}=\sum_{t=1}^{24}\left(\xi_{csp}^{SP}\cdot P_{csp}^{O}(t)+\xi_{csp}^{HS}\cdot\left(P_{st}^{IN}(t)+P_{st}^{OUT}(t)\right)\right) \tag{19}$$

$$C_{ele}^{RUN}=\sum_{t=1}^{24}\left(\xi_{ele}\cdot P_{ele}^{W}(t)\right) \tag{20}$$

$$C_{pur}=\sum_{t=1}^{24}\left(\beta_{grid}\cdot P_{grid}^{BUG}(t)\right) \tag{21}$$

$$C_{inc}=\sum_{t=1}^{24}\left(\beta^{O_2}\cdot Y_{ele}^{O_2}(t)\right) \tag{22}$$

The above equation, C_{total} is the total system cost. C_{inv} is the cost of equipment investment. C_{run} is the cost of equipment operation and maintenance. C_{pur} is the cost of purchasing electricity. C_{inc} benefits the cost of oxygen. P_{wind}, P_{pv}, P_{csp}, P_{ele} are wind power stations, photovoltaic power stations, concentrating solar power stations, and electrolyzer equipment power, kW. M^{H_2} is the volume of the hydrogen storage tank in the system, measured in cubic meters, m^3. C_{wind}^{INV}, C_{pv}^{INV}, C_{csp}^{INV}, C_{ele}^{INV} are respectively the investment costs of the wind power station, photovoltaic power station, concentrating solar power station, and electrolyzer, $CNY\cdot kW^{-1}$. C_{st}^{INV} is the investment cost of the storage tank, $CNY\cdot m^{-3}$. ξ_{wind}, ξ_{pv}, ξ_{ele} are respectively the unit operation and maintenance costs of a wind power station, a photovoltaic power station, and an electrolyzer, $CNY\cdot kW^{-1}$. ξ_{csp}^{SP} is the unit operation and maintenance cost of the turbine power generation for the concentrating solar power station, $CNY\cdot kW^{-1}$. ξ_{csp}^{HS} is the unit operation and maintenance cost of the turbine for power generation at the concentrating solar power station, and the unit is $CNY\cdot kW^{-1}$. $P_{ele}^{W}(t)$ is the operating power of the electrolyzer at time t, kW. $P_{wind}^{O}(t)$, $P_{pv}^{O}(t)$ are respectively the output power of a wind power station and a photovoltaic power station at time t, kW. β_{grid} is the unit price of electricity, $CNY\cdot kW^{-1}$. β^{O_2} is the unit price of oxygen, $CNY\cdot kW^{-1}$.

3.2. Constraint condition

(1) Constraints of wind power

Output power constraints of wind power systems:

$$P_{wind}^{MIN}\le P_{wind}^{O}(t)\le P_{wind}^{MAX} \tag{23}$$

The above equation, P_{wind}^{MAX}, P_{wind}^{MIN} represent the wind power station's maximum and minimum output power in kW.

(2) Constraints of photovoltaic power

Output power constraints of photovoltaic power systems:

$$P_{pv}^{MIN}\le P_{pv}^{O}(t)\le P_{pv}^{MAX} \tag{24}$$

The above equation, P_{pv}^{MAX}, P_{pv}^{MIN} indicate the maximum and minimum output power of photovoltaic power stations as kW.

(3) Constraints of battery

Output power constraints of battery systems:

$$P_{ch}^{MIN}\le P_{sb}^{CH}(t)\le P_{ch}^{MAX} \tag{25}$$

$$P_{disch}^{MIN}\le P_{sb}^{DISCH}(t)\le P_{disch}^{MAX} \tag{26}$$

$$P_{sb}^{MIN}\le P_{sb}^{S}\le P_{sb}^{MAX} \tag{27}$$

The above equation, P_{ch}^{MAX}, P_{disch}^{MAX} respectively indicate the maximum power of battery charging and discharging. The unit is kW. P_{ch}^{MIN}, P_{disch}^{MIN} respectively represent the minimum power for battery charging and discharging, kW. P_{sb}^{MAX}, P_{sb}^{MIN} respectively indicate the maximum and minimum power stored by the battery, kW.

(4) Constraints of concentrating solar power

Output power constraints of concentrating solar power station:

$$P_{csp}^{MIN} \le P_{csp}^{O}(t) \le P_{csp}^{MAX} \tag{28}$$

$$P_{csp}(t) - P_{csp}(t-1) \le P_{csp}^{UP} \tag{29}$$

$$P_{csp}(t-1) - P_{csp}(t) \le P_{csp}^{DOWN} \tag{30}$$

The above equation, P_{csp}^{MAX}, P_{csp}^{MIN} respectively represent the maximum and minimum power output of the concentrating solar power station, kW. P_{csp}^{UP}, P_{csp}^{UP} respectively represent the upper and lower limits of the output power range of the concentrating solar power station, kW.

(5) Thermal equilibrium constraints

$$P_{csp}^{U}(t) \ge 0 \tag{31}$$

$$0 \le P_{tur}^{IN}(t) \le \frac{P_{csp}^{MAX}}{\eta_{tc}} \tag{32}$$

(6) Constraints of thermal storage system

$$0 \le P_{hs}^{IN}(t) \le P_{hs}^{IM} \tag{33}$$

$$0 \le P_{hs}^{OUT}(t) \le P_{hs}^{OM} \tag{34}$$

$$0 \le P_{hs}^{S} \le \frac{\mu^{FULL} P_{csp}^{MAX}}{\eta_{tc}} \tag{35}$$

The above equation, P_{hs}^{IM}, P_{hs}^{OM} represent the maximum heat input and output of the heat storage system, kW. μ^{FULL} The variable represents the number of hours at full load of the nighttime concentrating solar power station, h.

4. Case Study

In the example studied in this paper, an alkaline electrolyzer with a capacity of 38 MW and an efficiency of 70% is utilized [28]. Oxygen is sold at 0.014 CNY·mol^{-1} [29]. The 24-h wind speed and solar resource data from a specific area in northern China are utilized. Tables 1–3 respectively provide the data necessary for the calculation. The wind speed and solar data are imported into MATLAB, and the output power can be calculated using the wind power output model and photovoltaic output model mentioned above, as illustrated in Fig. 4. The objective function is solved by the CPLEX solver to find the optimal hydrogen production scheme. The division of electricity prices [30]: The valley hours are 00:00–07:00 and 23:00–24:00. The normal hours are 07:00–10:00 and 15:00–18:00. Peak hours are 10:00–15:00, 18:00–21:00, and 21:00–23:00. The electricity pricing for the power grid is presented in Table 4.

Table 1
Main parameters of output and storage system of concentrating solar power station.

Parameter	Value	Parameter	Value
P_{csp}^{MAX}/kW	20750	ξ_{csp}^{SP}/CNY·kW^{-1} [31]	0.072
P_{csp}^{MIN}/kW	0	ξ_{csp}^{HS}/CNY·kW^{-1} [31]	0.032
η_{cs}	0.42	C_{csp}^{INV}/CNY·kW^{-1} [31]	23000
η_{tc} [32]	0.4	μ^{FULL}/h	12
η_{hl} [32]	0.01	P_{hs}^{IM}/kW	55824
η_{hs} [32]	0.03	P_{hs}^{OM}/kW	43054
η_{hs}^{IN} [32]	0.98	P_{csp}^{UP}/kW	30
η_{hs}^{OUT} [32]	0.98	P_{csp}^{DOWN}/kW	30

Table 2
Main parameters of wind power output, photovoltaic output, and electrolyzer cost.

Parameter	Value	Parameter	Value
C_{ele}^{INV}/CNY·kW^{-1} [33]	2000	P_{wind}^{MAX}/kW	18000
ξ_{ele}/CNY·kW^{-1} [28]	4%C_{ele}^{INV}	P_{wind}^{MIN}/kW	0
ξ_{wind}/CNY·kW^{-1} [34]	0.029	P_{pv}^{MAX}/kW	18000
ξ_{pv}/CNY·kW^{-1} [35]	0.031	P_{pv}^{MIN}/kW	0
C_{wind}^{INV}/CNY·kW^{-1} [16]	7410	η_{ch}、η_{disch} [24]	0.9
C_{pv}^{INV}/CNY·kW^{-1} [16]	3672	η_{ch}	0.001

Table 3
Other parameters.

Parameter	Value	Parameter	Value
C_{st}^{INV}/CNY·m^{-3} [36]	348400	P_{ch}^{MIN}/kW	0
P_{ch}^{MAX}/kW [37]	2680	P_{disch}^{MIN}/kW	0
P_{disch}^{MAX}/kW [37]	2680	P_{sb}^{MAX}/kW [37]	10719
P_{sb}^{MIN}/kW [37]	2680		

4.1. Capacity optimization configuration

In MATLAB, the CPLEX solver is invoked through the YALMIP platform to model and solve the designed renewable energy electrolytic water hydrogen production system. The specific solution process is shown in Fig. 5. At the beginning of the modeling process, an analysis was conducted to clarify the impact of wind turbine installed capacity, photovoltaic installed capacity, and concentrating solar power station installed capacity on the cost of the hydrogen production system. This involved exploring and

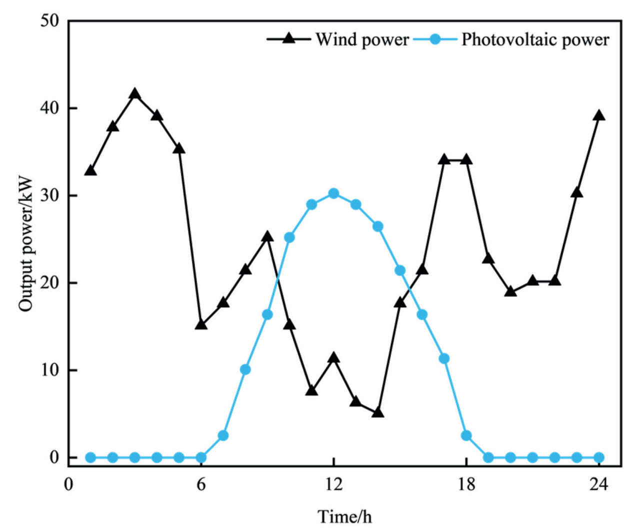

Fig. 4. Output power curve of a wind farm and a photovoltaic field.

Table 4
The time of electricity usage and the Corresponding prices from the power grid.

Period of time	Electricity price/CNY·(kW·h)$^{-1}$
Peak hours	0.83
Normal hours	0.49
Valley hours	0.17

analyzing wind power hydrogen production, photovoltaic hydrogen production, and concentrating solar power hydrogen production systems. Therefore, when programming and calculating, the installed capacity is set to 80 MW. The relationship between the installed capacity of different renewable energy power generation equipment and the cost of hydrogen production is determined by adjusting the capacity, as illustrated in Fig. 6.

From (a) in Fig. 6, it can be observed that when the installed capacity of each individual unit is 26 MW, 52 MW, 78 MW, 104 MW, and 156 MW, the cost of wind power hydrogen production decreased from 88.85 CNY·kg^{-1} to 19.94 CNY·kg^{-1}, the cost of photovoltaic hydrogen production decreased from 98.77 CNY·kg^{-1} to 66.71 CNY·kg^{-1}, and the cost of concentrating solar power hydrogen production decreased from 69.85 CNY·kg^{-1} to 38.95 CNY·kg^{-1}. From the calculation results, it can be analyzed that the cost of hydrogen production from wind power and concentrating solar power is lower than that of photovoltaic hydrogen production. This is mainly because wind power can generate electricity at night, while concentrating solar power storage systems store heat during the day and release it at night, reducing their reliance on the power grid. Photovoltaic power generation only produces electricity during the day; therefore, the system depends entirely on the power grid at night. As the installed capacity of individual wind, photovoltaic, and concentrating solar power units increases, the cost of electrolyzing water to produce hydrogen in renewable energy systems gradually decreases. The changing trend of photovoltaic power installed capacity and concentrating solar power installed capacity on hydrogen production cost is relatively similar, while the changing trend of wind turbine installed capacity is different. This difference is primarily attributed to the variance between wind energy resources and solar resources. From Fig. 6 (b), it can be seen that as the installed capacity of each unit increases from 26 MW to 156 MW, the hydrogen production cost of the system decreases, but the investment cost of the equipment increases significantly. The most obvious change is in concentrating solar power, primarily because the unit investment cost of equipment is much higher than that of wind power and photovoltaic. In various scenarios of renewable energy electrolysis of water hydrogen production systems, the hydrogen production in the electrolyzer system remains stable. According to the established mathematical model and provided parameters, further increasing the capacity of renewable energy equipment following the trend in Fig. 6 will lead to a gradual decrease in system costs. However, this decrease will not reach zero; instead, it will be followed by a significant increase in system investment costs. In the mentioned case, the capacity of the electrolyzer is 38 MW. If the maximum power generation of individual wind power, photovoltaic, and concentrating solar power units exceeds the power consumption of the electrolyzer, a significant surplus of electricity will be produced by the renewable energy system. Storing this excess electricity using batteries would result in high investment costs for the battery storage, which is not conducive to the economic viability of the system. Considering the investment cost of various renewable energy power generation equipment and other factors, the installed capacity of each power generation equipment should be allocated

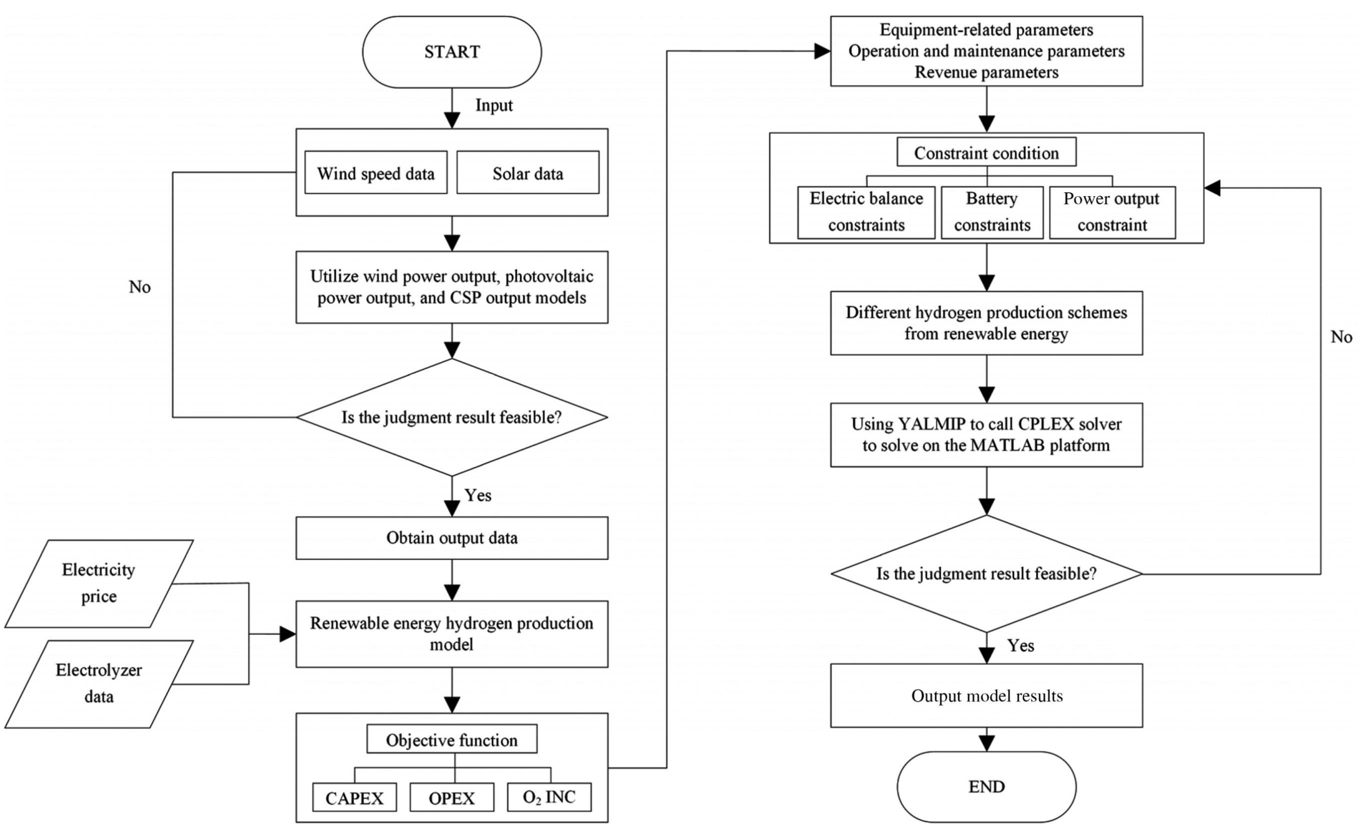

Fig. 5. Flow chart of capacity optimization configuration solution.

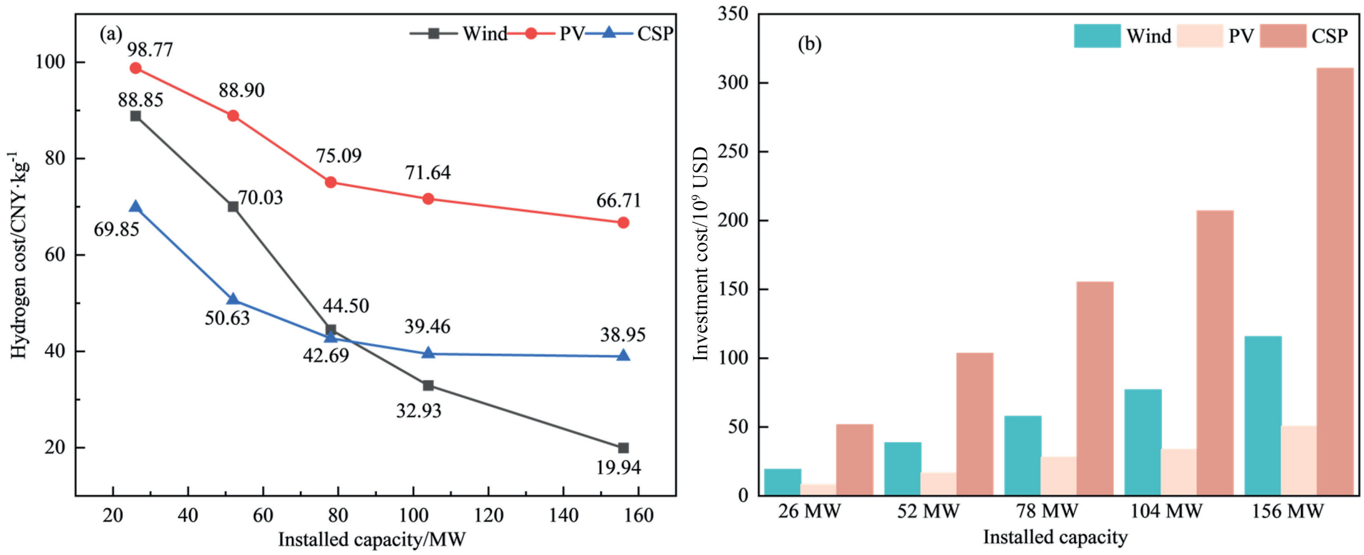

Fig. 6. Impact of installed capacity of renewable energy power generation equipment on costs in an independent hydrogen production system. (a) Impact of installed capacity on hydrogen production cost. (b) Impact of installed capacity on investment cost.

reasonably based on the compromise principle in each unique renewable energy electrolytic water hydrogen generation scheme. This approach aims to minimize the cost of hydrogen production.

In this paper, the capacity configuration of hydrogen production from renewable energy by electrolyzing water is analyzed under multiple scenarios. By formulating the objective function and constraint conditions in MATLAB, and utilizing the YALMIP platform to invoke the CPLEX solver for solutions, the capacity optimization setup for power generation equipment in hydrogen production from renewable energy electrolyzed water is achieved for each scenario.

Scenario 1: Hydrogen production from wind power

To enhance the utilization rate of renewable energy, the wind power hydrogen generation system needs to incorporate a battery energy storage system. After programming in MATLAB and adjusting the installed capacity of the wind farm, the output power results for each module are obtained through a comprehensive comparative analysis, as illustrated in Fig. 7. It can be seen from the figure that when only wind power is used in the renewable energy hydrogen generation system, it is necessary to purchase some electricity from the grid to ensure the smooth operation of the electrolyzer. The output power of wind power generation fluctuates between peak and valley values. When the output power exceeds the operational power of the electrolyzer, the surplus power will be stored in the battery. When the output power of wind power generation cannot meet the system demand, the battery will discharge to maximize the utilization of wind energy resources.

The software calculates and analyzes the energy flow of the generator set and the hydrogen production of the electrolyzer in the wind power hydrogen generation system, as depicted in Fig. 8. It can be seen from the results in the figure that the total power generation of the wind farm in the wind power hydrogen generation system in a day is 501179.98 kW·h. The storage capacity of the battery is 11512.68 kW·h, the unused power of the system is 2809.74 kW·h, and the renewable energy utilization rate is 99.44%. These results indicate that the capacity configuration of the renewable energy side of the wind power hydrogen generation system is reasonable. After optimization calculations, the installed capacity of the fan is 104 MW, and the capacity of the battery is 10.8 MW. Due to the fluctuating nature of wind power output,

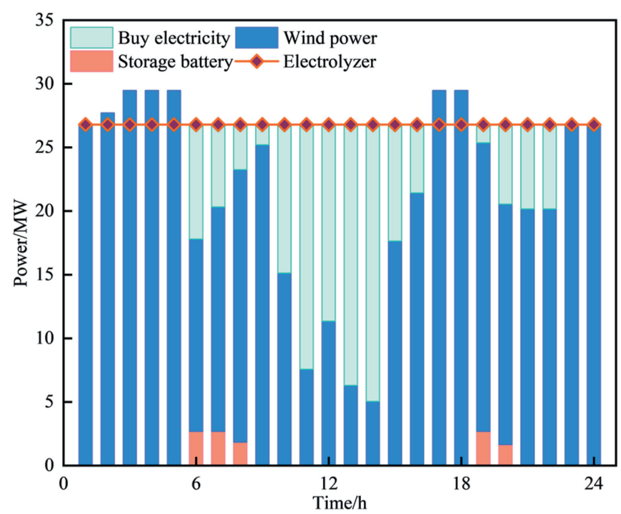

Fig. 7. Output of each module in a wind power hydrogen generation system.

renewable energy cannot provide a stable input for the electrolyzer power. To ensure the smooth operation of the electrolyzer, the grid needs to supply 144716.58 kW·h of electricity, achieving a renewable energy penetration rate of 78% for the wind power hydrogen generation system.

Scenario 2: Photovoltaic hydrogen production

In the photovoltaic hydrogen generation system, integrating a battery energy storage system is essential to enhance the utilization rate of renewable energy. According to MATLAB programming, the output power results for each module are obtained through a comprehensive comparative analysis by adjusting the installed capacity of the photovoltaic field, as illustrated in Fig. 9. It can be seen from the results in the figure that although the photovoltaic hydrogen generation system requires minimal purchased electricity during the day, the photovoltaic output is zero at night. Therefore, the electrolyzer's operational power needs can only be met by purchasing electricity from the grid. When the photovoltaic output exceeds the operational capacity of the electrolyzer, the excess

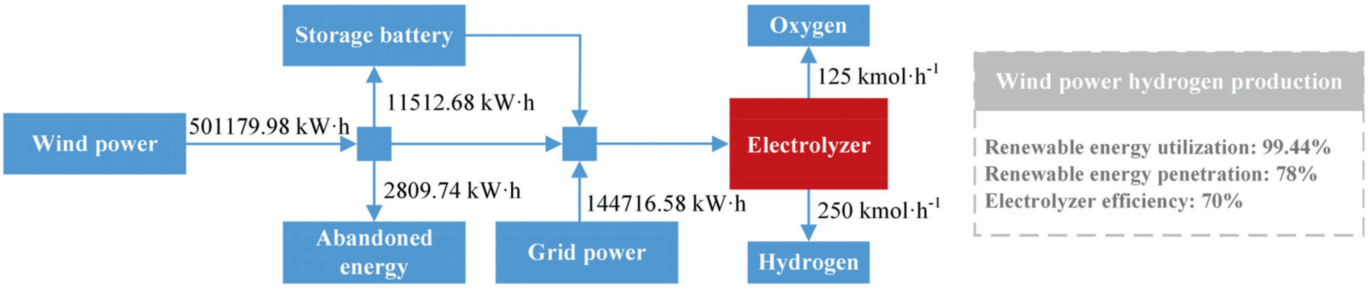

Fig. 8. Energy flow and logistics of wind power hydrogen generation system.

power will be stored in the battery. When the photovoltaic output cannot meet the system's demand, the battery will discharge.

The software calculates and analyzes the energy flow of the generator set and the hydrogen production of the electrolyzer in the photovoltaic hydrogen generation system, as illustrated in Fig. 10. It can be observed from the results in the figure that the power generation of the photovoltaic field in the photovoltaic hydrogen generation system in a day is 239701.83 kW·h. The storage capacity of the battery is 7192.98 kW·h, with 1791.214 kW·h of power being abandoned by the system. The utilization rate of renewable energy is 99.25%, indicating that the capacity configuration of the renewable energy side of the photovoltaic hydrogen generation system is reasonable. After the optimization calculation, the installed PV capacity of the system is 92 MW, and the battery capacity is 27.6 MW. Since the photovoltaic power station only operates during the daytime and ceases to generate electricity at night, the grid must

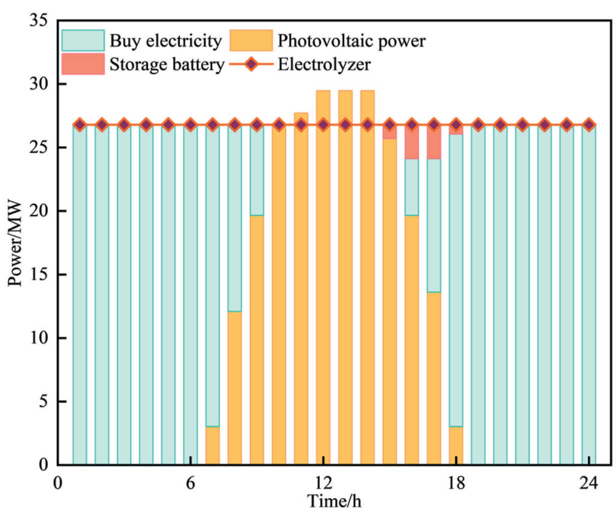

Fig. 9. Output of each module in the photovoltaic hydrogen generation system.

supply 405176.21 kW·h of electricity to ensure the smooth operation of the electrolyzer, leading to a 37% penetration rate of renewable energy.

Scenario 3: Concentrating solar power hydrogen production

The renewable energy generated by the concentrating solar power hydrogen generation system is solely from concentrating solar power generation. Due to the presence of a heat storage system unit in the concentrating solar power generation system, there is no requirement to incorporate a battery into the system. According to MATLAB programming, modifying the installed capacity of the optical thermal power station allows for obtaining the output power results between each unit after a comprehensive comparative analysis, as shown in Fig. 11. It can be seen from the figure that the output power of the concentrating solar power station can meet the 24-h operation of the electrolyzer, and there is no purchased power in the system. The heat storage tank unit in the concentrating solar power station stores heat during the day and provides it to the steam turbine for power generation at night. The heat stored in the heat storage tank can also be used to power the hydrogen production system in the morning and evening.

The software calculates and analyzes the energy flow of the generator set and the hydrogen production of the electrolyzer in the concentrating solar power hydrogen generation system, as illustrated in Fig. 12. It can be seen from the results in the figure that the power generation capacity of the concentrating solar power station in a day is 643086.82 kW·h. The abandoned power of the system is 0.004 kW·h, and the utilization rate of renewable energy is 99.99%. These results indicate that the capacity configuration of the renewable energy side in the concentrating solar power hydrogen generation system is reasonable. After optimizing the calculations, the installed capacity of the concentrating solar power station in the system is 170 MW. Since the concentrating solar power station can continuously and stably supply power to the electrolyzer to produce hydrogen, the grid's power purchase in the system is 0 kW·h, resulting in a 100% penetration rate of renewable energy.

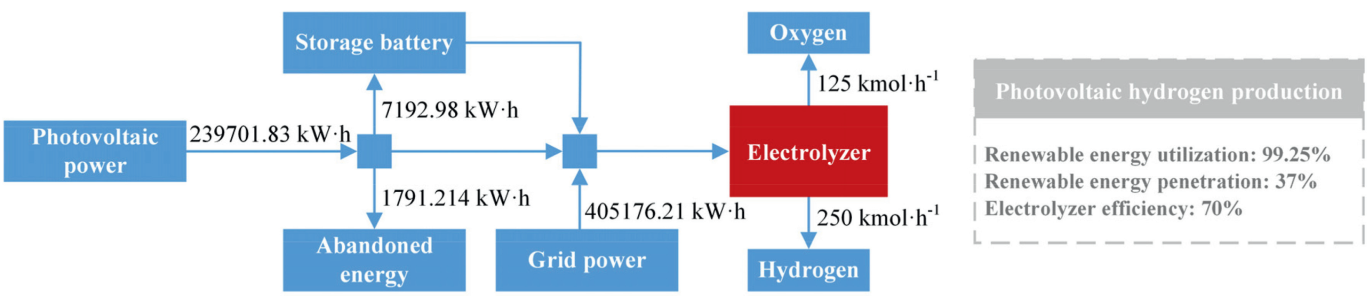

Fig. 10. Energy flow and logistics of photovoltaic hydrogen generation system.

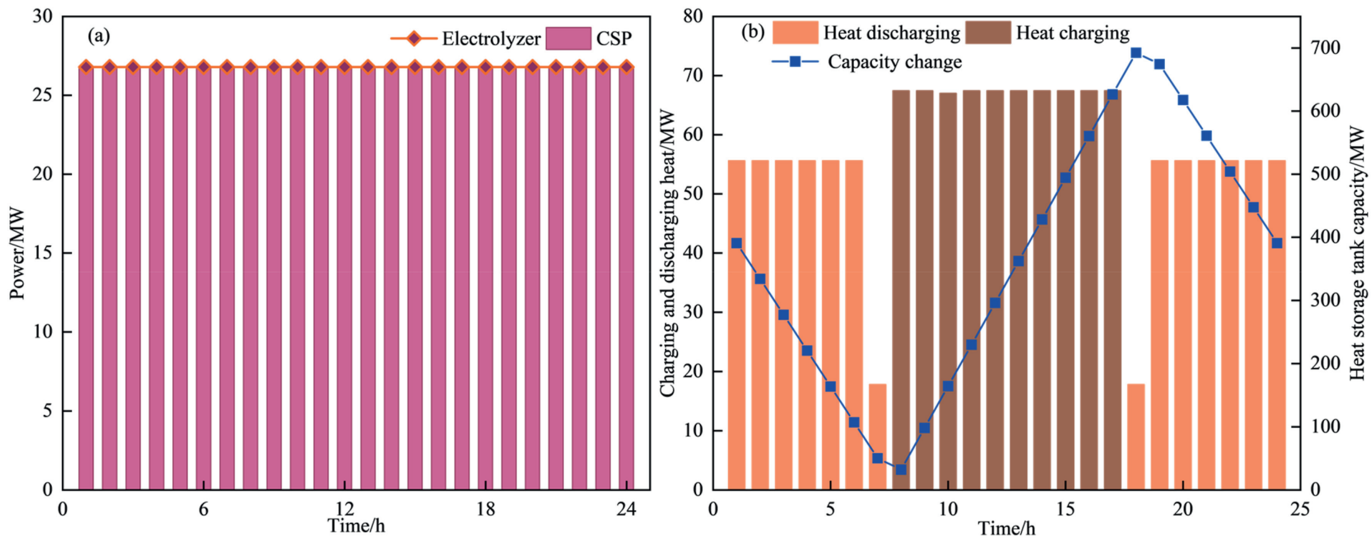

Fig. 11. Output of each unit of concentrating solar power hydrogen generation system. (a) Output results of each unit in the system. (b) Change of charging and discharging heat and capacity of heat storage tank.

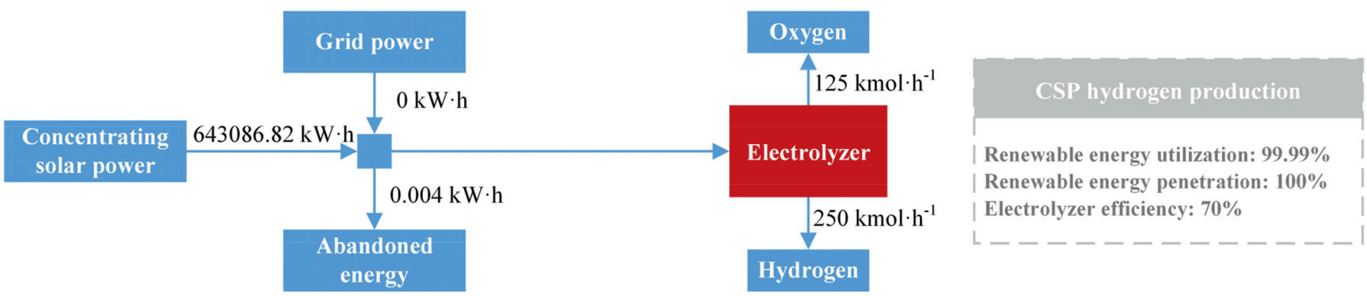

Fig. 12. Energy flow and logistics of concentrating solar power hydrogen production system.

Scenario 4: Hydrogen production by wind-PV coupling

The renewable energy aspect of the wind-PV coupling hydrogen generation system comprises wind power generation, photovoltaic power generation, and storage battery. According to MATLAB programming, by adjusting the installed capacity of each unit in the renewable energy side of the wind-PV coupling hydrogen generation system, the output power results for each unit are obtained through a comprehensive comparative analysis, as illustrated in Fig. 13. It can be seen from the figure that photovoltaic power generation and wind power generation during the day in the wind-PV coupling hydrogen generation system can meet the power consumption of the electrolyzer, reducing the cost of purchased power for the system. Compared with hydrogen production from wind power or photovoltaics, the installed capacity is greatly reduced. At night, the system can only rely on wind power output and partial battery discharge, requiring it to purchase electricity from the grid.

The software calculates and analyzes the energy flow of the generator set and the hydrogen production of the electrolyzer in the wind-PV coupling hydrogen production system, as illustrated in Fig. 14. It can be seen from the results in the figure that the power generation capacity of the wind farm, photovoltaic field, storage battery, and unused power of the wind-PV coupling hydrogen generation system is 370181.5 kW·h, 170371.93 kW·h, 7371.4 kW·h, and 1832.144 kW·h respectively. After calculation, the utilization rate of renewable energy is 99.66%, indicating that the capacity configuration of renewable energy in the wind-PV coupling hydrogen generation system is reasonable. After optimization calculations, the installed capacities of the wind turbine, photovoltaic system, and storage battery are 67 MW, 34 MW, and 10.5 MW, respectively. The integration of wind farms and photovoltaic fields has decreased the grid's power purchase to 104365.53 kW·h, resulting in an increased renewable energy

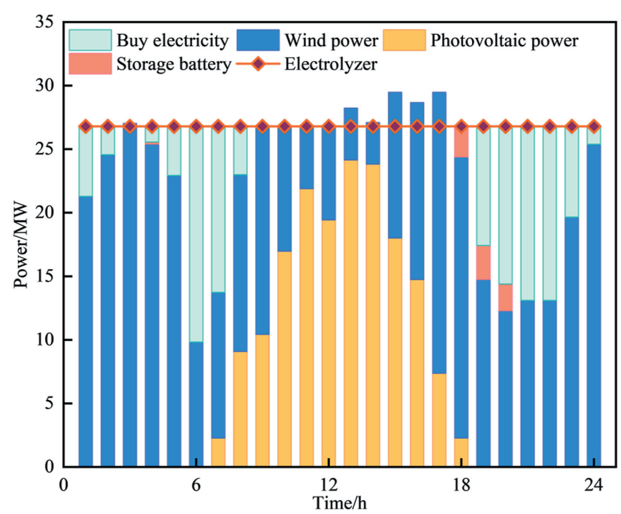

Fig. 13. Output of each unit in the wind-PV coupling hydrogen production system.

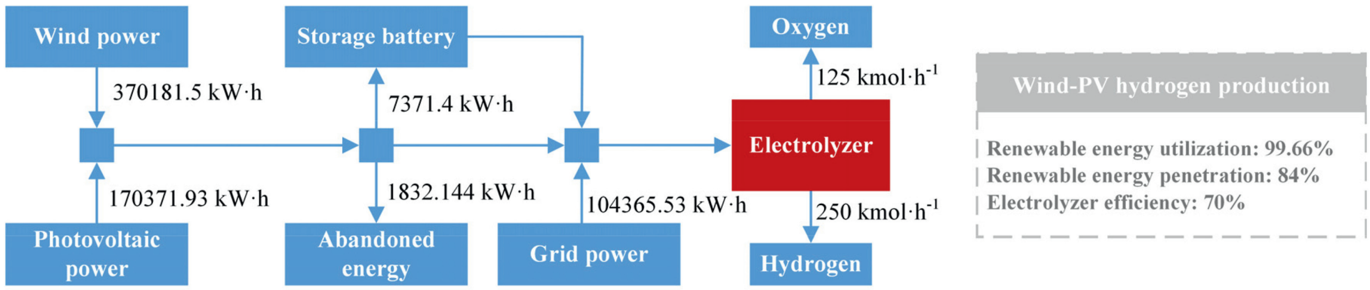

Fig. 14. Energy flow and logistics of wind-PV coupling hydrogen production system.

penetration rate of 84%. By comparing the hydrogen production systems of wind power and photovoltaics, it is evident that the penetration rate of renewable energy in the wind-PV coupling system is higher.

Scenario 5: PV-CSP coupling hydrogen production

The PV-CSP coupling system involves integrating a photovoltaic field with concentrating solar power for hydrogen production. According to MATLAB programming, by adjusting the installed capacity of each unit in the renewable energy side of the PV-CSP coupling hydrogen production system, the output power results for each unit are obtained after a comprehensive comparative analysis, as illustrated in Fig. 15. It can be seen from the figure that in the PV-CSP coupling hydrogen production system, the system mainly relies on photovoltaic power generation to provide working power to the electrolyzer during the day, and is entirely supplied by the concentrating solar power station at night. Renewable energy can smoothly power the electrolyzer, eliminating the need for purchased electricity in the system. Photovoltaic power generation complements concentrating solar power generation during the day. The heat storage tank system stores excess heat and smoothly provides heat to the steam turbine for power generation at night.

The energy flow of the generator set and the hydrogen production of the electrolyzer in the PV-CSP coupling hydrogen production system are calculated and analyzed by software, as shown in Fig. 16. It can be seen from the results in the figure that the power generation capacity of the photovoltaic field in the PV-CSP coupling hydrogen generation system in a day is 212685.86 kW·h, the power generation capacity of the concentrating solar power station is 430400.97 kW·h, and the unused power of the system is 0.014 kW·h. After calculation, the utilization rate of renewable energy is 99.99%, indicating that the capacity configuration of the renewable energy side in the PV-CSP coupling hydrogen generation system is reasonable. After optimization calculations, the installed capacity of the photovoltaic system is 34 MW, while the scale of the concentrating solar power station is 84 MW. Since renewable energy can fully meet hydrogen production through electrolysis, the electricity purchased from the power grid is 0 kW h, resulting in a 100% penetration rate of renewable energy.

Scenario 6: Hydrogen production by wind-PV-CSP coupling

The wind-PV-CSP coupling hydrogen production system is an extension of the wind-PV coupling hydrogen production system. It incorporates a concentrating solar power station while eliminating the need for a battery. According to MATLAB programming, by adjusting the installed capacity of each unit in the renewable energy side of the wind-PV-CSP coupling hydrogen generation system, the output power results for each unit are obtained after a comprehensive comparative analysis, as illustrated in Fig. 17. It can be seen from the figure that the wind-PV-CSP coupling hydrogen generation system does not purchase electricity from outside the grid system, which fully meets the power requirements of the electrolyzer in the system. Compared with wind-power hydrogen production, photovoltaic hydrogen production, and wind-PV

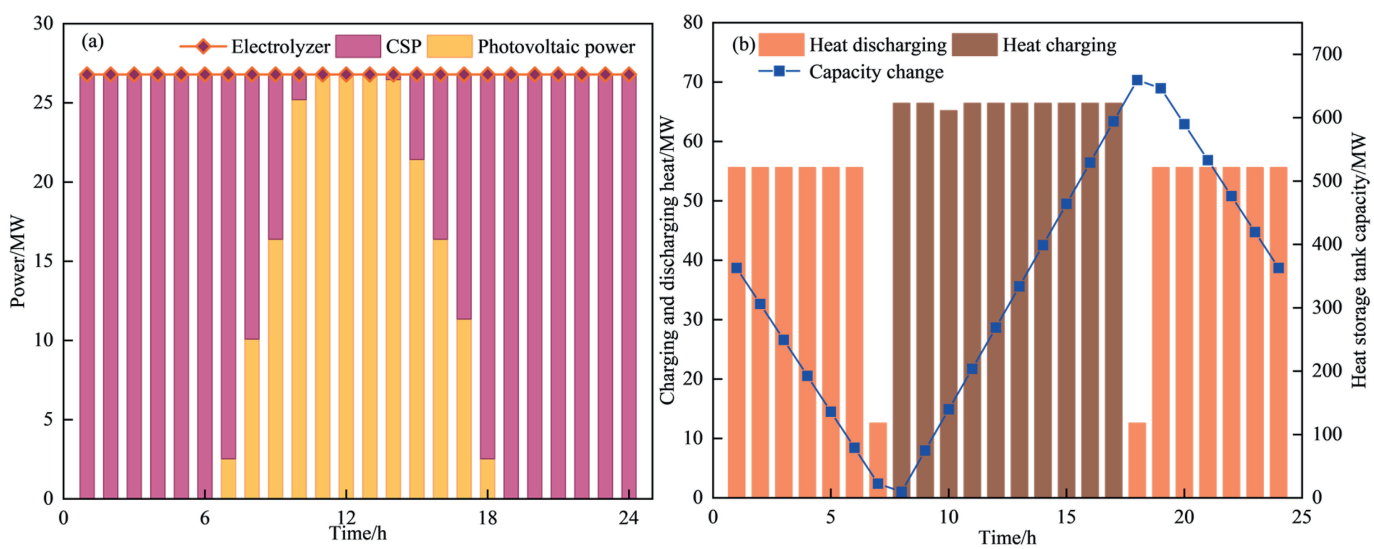

Fig. 15. Output of each unit of PV-CSP coupling hydrogen production system. (a) Output results of each unit in the system. (b) Change of charging and discharging heat and capacity of heat storage tank.

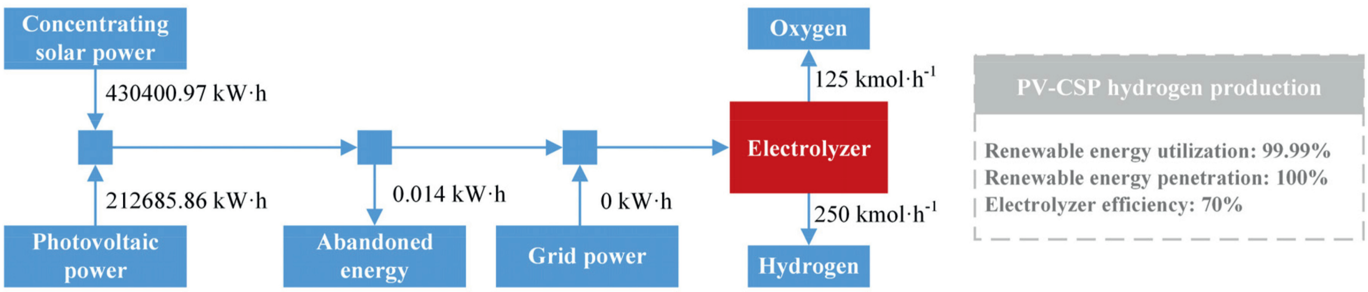

Fig. 16. Energy flow and logistics of PV-CSP coupling hydrogen production system.

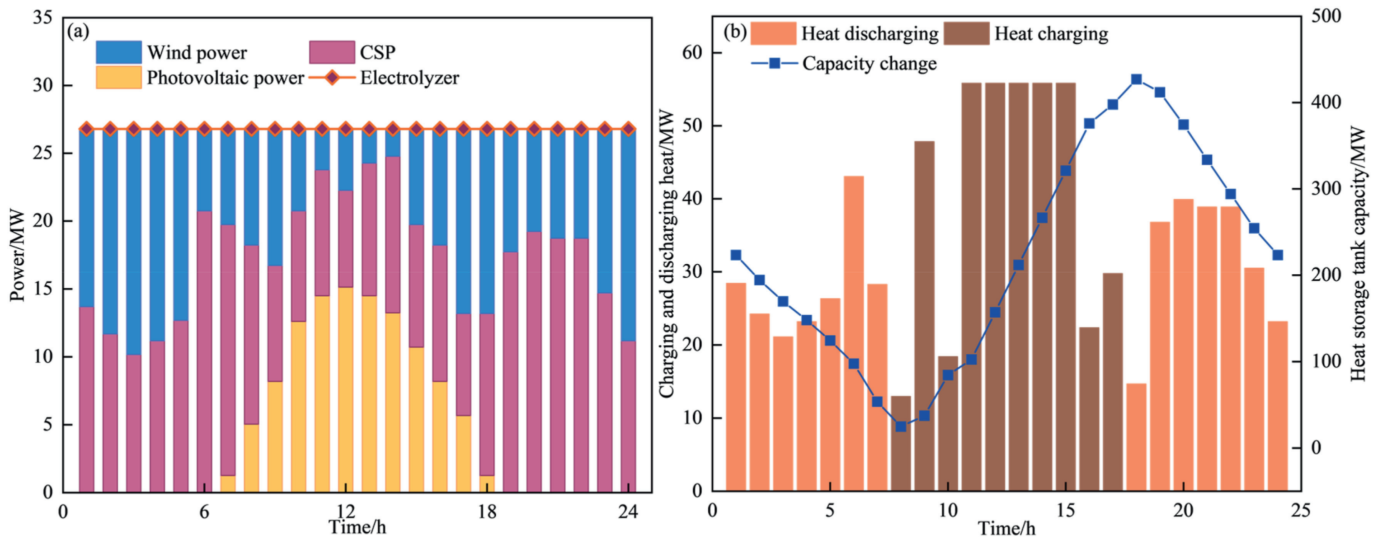

Fig. 17. Output of each unit of wind-PV-CSP coupling hydrogen production system. (a) Output results of each unit in the system. (b) Change results of charging and discharging heat power and capacity of heat storage tank.

coupling hydrogen production, the purchased power in the system is reduced. For concentrating solar power hydrogen production and PV-CSP coupling hydrogen production, the system significantly reduces the size of the photothermal power station. The heat storage system in the concentrating solar power station stores heat during the day releases it at night, and, in conjunction with the wind farm, provides electrical energy to the electrolytic cell to reduce the amount of purchased power in the system.

The software calculates and analyzes the energy flow of the generator set and hydrogen production of the electrolyzer cell in the wind-PV-CSP coupling hydrogen production system, as illustrated in Fig. 18. It can be seen from the figure that the wind farm power generation of the wind-PV-CSP coupling hydrogen generation system is 227804 kW·h, the photovoltaic field power generation is 110250 kW·h, the concentrating solar power station power generation is 305032.82 kW·h, and the unused power of the system is 0.004 kW·h. After calculation, the utilization rate of renewable energy is 99.99%, indicating that the capacity configuration of the renewable energy side in the wind-PV-CSP coupling hydrogen generation system is reasonable. After the optimization calculation, the installed capacity of a wind turbine is set at 42 MW, the installed capacity of PV is set at 20 MW, and the scale of the concentrating solar power station is set at 69 MW. The combination of wind, photovoltaic (PV), and concentrated solar power (CSP)

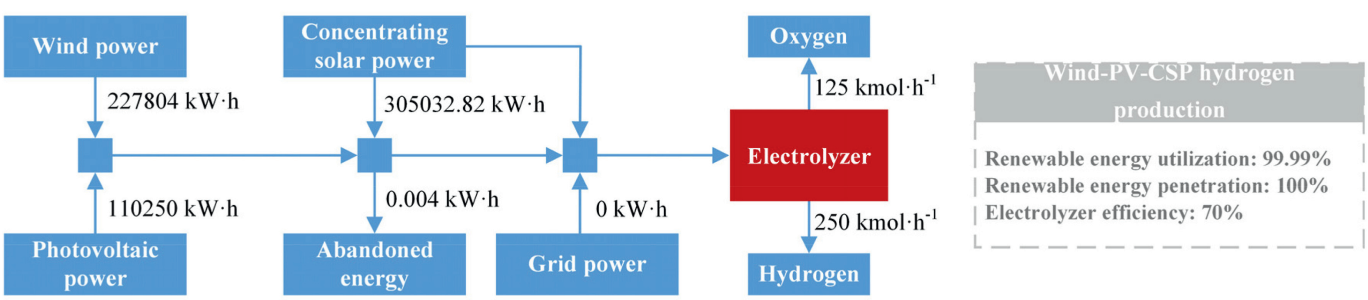

Fig. 18. Energy flow and logistics of wind-PV-CSP coupling hydrogen production system.

renewable energy sources can fully meet the power consumption of the electrolyzer, resulting in a 100% penetration rate of renewable energy in the system.

4.2. Economic analysis

The target values for wind power hydrogen production, photovoltaic hydrogen production, concentrating solar power hydrogen production, wind-PV coupling hydrogen production, PV-CSP coupling hydrogen production, and wind-PV-CSP coupling hydrogen production are calculated using MATLAB. The hydrogen production cost of each system and the proportion of output power of each unit are shown in Fig. 19. It can be seen from the figure that the cost of hydrogen production from wind power is 32.93 CNY·kg^{-1}, and the power purchase ratio in the system is 22%. The cost of photovoltaic hydrogen production is 72.13 CNY·kg^{-1}, and the proportion of system power purchase is 62.1%. The cost of hydrogen production through wind-PV coupling is 25.86 CNY·kg^{-1}, and the system purchases 16% of the power. After the wind-PV coupling, not only is the proportion of power purchased by the grid reduced, but the cost of hydrogen production is also significantly lower compared to that of wind power and photovoltaic hydrogen production. The cost of concentrating solar power hydrogen production is 48.42 CNY·kg^{-1}, and the system does not require purchased electricity. The cost of PV-CSP coupled hydrogen production is 25.78 CNY·kg^{-1}, and the system does not require purchased electricity. The cost of hydrogen production after coupling PV with CSP is significantly lower than that of concentrating solar power hydrogen production. The cost of hydrogen production through wind-PV-CSP coupling is 18.84 CNY·kg^{-1}, and there is no purchased power in the system. The system contemplates integrating concentrating solar power with wind-PV coupling for hydrogen production, resulting in a reduced cost of hydrogen production. To sum up, the cost of hydrogen production through wind-PV-CSP coupling is the lowest and holds greater development prospects.

At present, the efficiency of concentrating solar power stations is about 16%, and the power generation cost of the concentrating solar power station is high. Therefore, the integration of concentrating solar power will result in a high cost of hydrogen production. According to relevant literature [38–40], concentrating solar power has attracted increasing attention, and the efficiency of concentrating solar power is projected to reach about 40% in the future. Therefore, this paper predicts the future costs of concentrating solar power hydrogen production, PV-CSP coupling hydrogen production, and wind-PV-CSP coupling hydrogen production. The results are shown in Fig. 20. In the future, the cost of concentrating solar power hydrogen production may be reduced to 35.30 CNY·kg^{-1}, the cost of PV-CSP coupling hydrogen production may be reduced to 19.23 CNY·kg^{-1}, and the cost of wind-PV-CSP coupling hydrogen production may be reduced to 16.02 CNY·kg^{-1}.

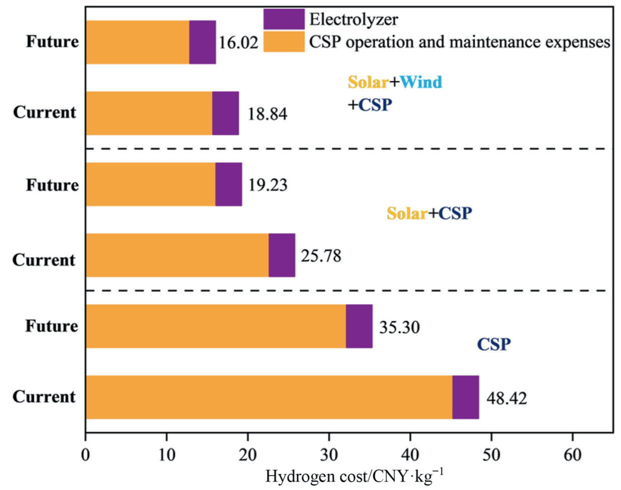

Fig. 20. Cost prediction of future CSP hydrogen production, PV-CSP coupling hydrogen production, and wind-PV-CSP coupling hydrogen production.

4.3. Comprehensive evaluation

The capacity configuration, investment cost, and hydrogen production cost under different scenarios are shown in Table 5 below. The installed capacity of the wind-PV coupling hydrogen generation system is 67 MW, with the photovoltaic capacity being 34 MW. Compared with wind power hydrogen generation and

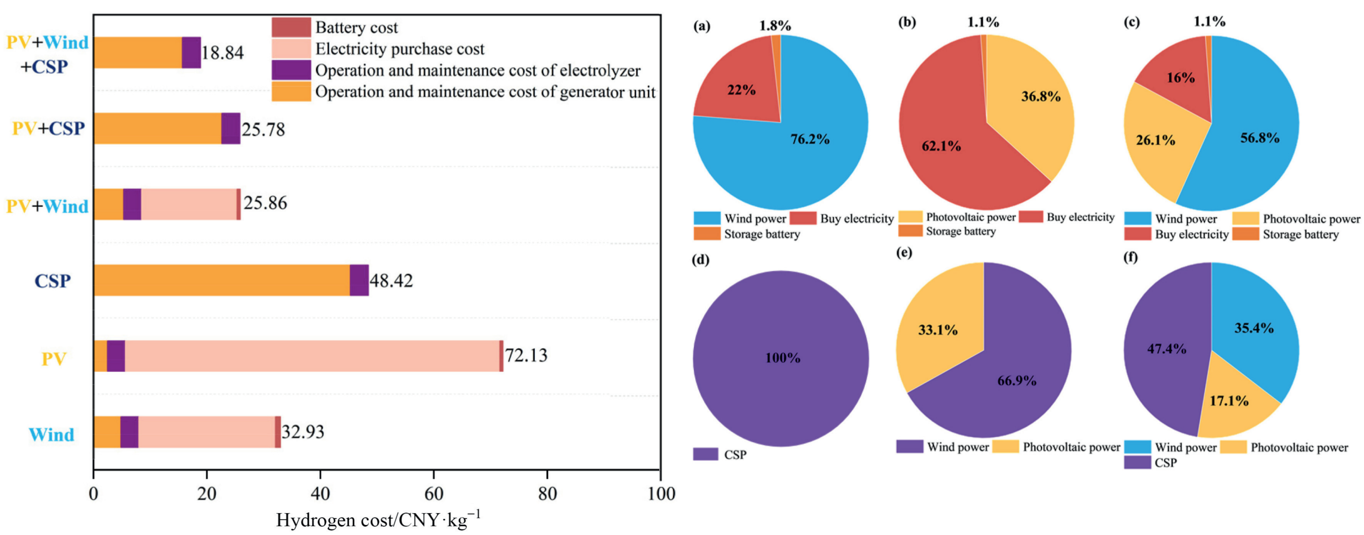

Fig. 19. Cost of hydrogen production systems from various renewable energy sources and the proportion of output power from each unit. (a) Output ratio of each unit of wind power hydrogen generation system. (b) Proportion of output from each unit of a photovoltaic hydrogen generation system. (c) Output ratio of each unit in a wind-PV coupled hydrogen generation system. (d) Output ratio of each unit of a concentrating solar power hydrogen generation system. (e) Proportion of output from each unit of a PV-CSP coupled hydrogen production system. (f) Output ratio of each unit of a wind-PV-CSP coupled hydrogen production system.

Table 5
Results of capacity allocation, investment costs, and hydrogen production costs under different scenarios.

	Installed capacity of wind/MW	Installed capacity of PV/MW	Battery capacity/MW	Installed capacity of CSP/MW	Investment cost/CNY	Hydrogen production cos/CNY·kg^{-1}	Renewable energy penetration/%	Renewable energy utilization/%
Scenario 1	104	–	10.8	–	8.598×10^8	32.93	78	99.44
Scenario 2	–	92	27.6	–	4.388×10^8	72.13	37	99.25
Scenario 3	–	–	–	170	3.98×10^9	48.42	100	99.99
Scenario 4	67	34	10.5	–	5.852×10^8	25.86	84	99.66
Scenario 5	–	34	–	84	2.138×10^9	25.78	100	99.99
Scenario 6	42	20	–	69	2.053×10^9	18.84	100	99.99

photovoltaic hydrogen generation, the capacity of the generator unit is reduced by about half. After integration, the adoption rate of renewable energy increased to 83.77%, marking a 46.77% increase compared to photovoltaic hydrogen production. This significantly decreased reliance on the power grid, and the cost of hydrogen production decreased to 25.86 CNY·kg^{-1}. PV-CSP coupling for hydrogen production involves integrating photovoltaic power generation into the concentrating solar power hydrogen production model. The results show that the scale of the concentrating solar power station is 84 MW, which significantly reduces the investment cost of equipment. With the integration of a concentrating solar power station, the renewable energy penetration rate has reached 100%, as determined by the operational characteristics of such a station. Compared with hydrogen production solely from renewable energy sources, hydrogen production from renewable energy coupling reduces the capacity of generating units and the investment cost of equipment. It also enhances the penetration and economic viability of renewable energy within the system. The wind-PV-CSP coupling hydrogen production considers wind power in conjunction with PV-CSP for hydrogen production. In the calculation results, the scale of the generator set, the investment cost (2.053×10^9 CNY), and the hydrogen production cost of system (18.84 CNY·kg^{-1}) are the lowest, indicating a promising development prospect. According to the Refs. [41,42], when wind speed and solar energy resources in an area are not optimal, and the wind turbine installation location is elevated, the area suitable for concentrating solar power generation is extensive. Considering various factors, photovoltaic and concentrating solar power generation primarily depend on solar energy resources, which are unrelated to wind speed. Therefore, coupling PV-CSP for hydrogen production should be developed in areas abundant in solar energy resources. Concentrating solar power generation has high terrain requirements. Therefore, in regions with flat terrain and ample wind and solar resources, it is advisable to develop hydrogen production through wind-PV-CSP coupling. The high terrain is suitable for the development of wind-PV coupled hydrogen production.

5. Conclusions

This article is based on a proposed model for optimizing the capacity of a renewable energy hydrogen production system. The model integrates wind power, photovoltaic (PV) power, and concentrating solar power (CSP) with an alkaline electrolyzer. With the aim of minimizing the total cost on a daily basis, the capacity optimization configuration and hydrogen production cost calculation of renewable energy electrolysis of water hydrogen systems under various scenarios were solved using the CPLEX solver. Through comprehensive analysis and comparison, it has been found that, compared to single renewable energy hydrogen production, the renewable energy coupling hydrogen production system reduces the capacity of generating units and the investment cost of equipment. This system also enhances the penetration and economic viability of renewable energy within the system. Notably, the cost of hydrogen production from wind-PV-CSP coupling is the lowest at 18.84 CNY·kg^{-1}, indicating greater development prospects.

(1) The capacity configuration of generator units in wind-power hydrogen production, photovoltaic hydrogen production, concentrating solar power hydrogen production, wind-PV coupling hydrogen production, PV-CSP coupling hydrogen production, and wind-PV-CSP coupling hydrogen production systems is optimized to achieve a renewable energy utilization rate exceeding 99%.

(2) Compared with wind power hydrogen generation and photovoltaic hydrogen generation, the capacity of the wind-PV coupling hydrogen generation unit is reduced by about half. After coupling, the renewable energy penetration rate reaches 84%, which is a 47% increase compared to photovoltaic hydrogen generation. This significantly reduces dependence on the power grid, and the cost of hydrogen production is also reduced to 25.86 CNY·kg^{-1}.

(3) The integration of photovoltaic (PV) technology with concentrating solar power (CSP) systems for hydrogen production leads to a reduction in the scale of CSP facilities. This integration results in a cost of hydrogen production amounting to 25.78 CNY·kg^{-1}. Compared to hydrogen production singly from renewable energy sources, utilizing renewable energy coupling for hydrogen production decreases the capacity requirements of generation units, lowers equipment investment costs, and enhances the integration and economic viability of renewable energy within the system.

(4) The capacity, equipment investment cost, and hydrogen production cost of the generator set in the wind-PV-CSP coupling hydrogen production system are the lowest, resulting in a cost of 18.84 CNY·kg^{-1} of hydrogen. With the continuous enhancement of CSP efficiency, the cost of hydrogen production using wind-PV-CSP technology is projected to decrease to 16.02 CNY·kg^{-1}, indicating promising development prospects.

In the renewable energy electrolysis of water system analyzed in this article for multiple scenarios, the hydrogen production in the electrolyzer system remains stable. As a result, the surplus electricity in the renewable energy system is relatively low, which does not impact the system's overall cost. The constructed mathematical model can also be applied to fluctuating hydrogen production. However, adjusting the hydrogen production in the electrolyzer based on the demand for hydrogen load will impact the penetration rate and utilization rate of renewable energy. When there is excess unused electricity, consideration should be given to storing it in batteries or integrating it into the grid to enhance system economics and decrease production costs. In the future, it is of great significance for the safe and stable operation of the entire renewable energy electrolysis of water hydrogen production system.

CRediT Authorship Contribution Statement

Huairong Zhou: Writing – review & editing, Project administration, Investigation, Funding acquisition. Xin Wu: Writing – original draft, Software, Methodology, Investigation. Chunlei Li: Supervision, Conceptualization. Siyu Yang: Project administration, Funding acquisition, Conceptualization. Zhichen Chen: Investigation, Data curation. Jun Lu: Validation, Software. Chen Fang: Resources, Data curation.

Declaration of Competing Interest

The authors declare that they have no known competing financial interests or personal relationships that could have appeared to influence the work reported in this paper.

Acknowledgements

This research was funded by Major Science and Technology Projects of Gansu Province (23ZDGF002), Hongliu Outstanding Youth Support Program of Lanzhou University of Technology (02-062212), and the Joint Funds of the National Natural Science Foundation of China (U22A20415).

Nomenclature

C_{inc}	system income
C_{inv}	equipment investment cost
C_{pur}	electricity purchasing cost
C_{run}	equipment running costs
C_{total}	total system cost
D	sunlight intensity
P^{G}_{csp}	thermal power gathered by the mirror field in CSP
P^{O}_{csp}	output power of CSP
P^{U}_{csp}	CSP unused power
P^{W}_{ele}	working power of the electrolyzer
P^{BUG}_{grid}	grid buys power
P^{IN}_{hs}, P^{OUT}_{hs}	input and output power of thermal storage system
P^{S}_{hs}	thermal storage system thermal storage power
P^{O}_{pv}	photovoltaic output power
P^{R}_{pv}	photovoltaic rated power
P^{CH}_{sb}, P^{DISCH}_{sb}	charging and discharging power of the battery
P^{S}_{sb}	battery electric storage capacity
P^{CON}_{tur}	consumption power of Steam turbine
P^{IN}_{tur}	input power of steam turbine
P^{STA}_{tur}	starting power of steam turbine
P^{O}_{wind}	wind power output power
P^{R}_{wind}	rated power of wind power
S_{mf}	area of the mirror field
v	wind speed
v^{I}	cut-in wind speed
v^{O}	cut-out wind speed
v^{R}	rated wind speed
$Y^{H_2}_{ele}$	hydrogen production in the electrolyzer
Γ	actual absorbed radiation
η_{ch}, η_{disch}	charging and discharging efficiency of battery
η_{cs}	photothermal conversion efficiency
η_{hl}	heat loss efficiency during the heat transfer process
η_{hs}	heat loss efficiency of thermal storage system
η^{IN}_{hs}, η^{OUT}_{hs}	thermal efficiency of input and output heat
η^{L}_{sb}	battery loss rate
η_{tc}	thermal electric conversion efficiency
κ	temperature coefficient
ξ_{pv}	photovoltaic running costs
ξ_{wind}	wind running costs

References

[1] A.O.M. Maka, M. Mehmood, Green hydrogen energy production: current status and potential, *Clean Energy* 8 (2) (2024) 1–7.
[2] J.R. Li, J. Lin, J.Y. Xiao, Y.H. Song, Y. Teng, Q. Gao, J. Song, Technical and energy consumption comparison of power-to-chemicals (P2X) technologies for renewable energy integration, *Journal of Global Energy Interconnection* 3 (1) (2020) 86–96.
[3] M. Groll, Can climate change be avoided? Vision of a hydrogen-electricity energy economy, *Energy* 264 (2023) 126029.
[4] P. Nikolaidis, A. Poullikkas, A comparative overview of hydrogen production processes, *Renew. Sustain. Energy Rev.* 67 (2017) 597–611.
[5] B.S. Zainal, P.J. Ker, H. Mohamed, H.C. Ong, I.M.R. Fattah, S.M.A. Rahman, L.D. Nghiem, T.M. Indra Mahlia, Recent advancement and assessment of green hydrogen production technologies, *Renew. Sustain. Energy Rev.* 189 (2024) 113941.
[6] B.E. Lebrouhi, J.J. Djoupo, B. Lamrani, K. Benabdelaziz, T. Kousksou, Global hydrogen development - a technological and geopolitical overview, *Int. J. Hydrogen Energy* 47 (11) (2022) 7016–7048.
[7] Q. Hassan, I.S. Abdulrahman, H.M. Salman, O.T. Olapade, M. Jaszczur, Techno-economic assessment of green hydrogen production by an off-grid photovoltaic energy system, *Energies* 16 (2) (2023) 744.
[8] Y.F. Li, X.P. Shi, H. Phoumin, A strategic roadmap for large-scale green hydrogen demonstration and commercialisation in China: a review and survey analysis, *Int. J. Hydrogen Energy* 47 (58) (2022) 24592–24609.
[9] M.K. Abbas, Q. Hassan, V.S. Tabar, S. Tohidi, M. Jaszczur, I.S. Abdulrahman, H. M. Salman, Techno-economic analysis for clean hydrogen production using solar energy under varied climate conditions, *Int. J. Hydrogen Energy* 48 (8) (2023) 2929–2948.
[10] R.D. Zhang, X.L. Xu, Y.H. Zhang, Y. Dong, Analysis and forecast of the substitution potential of China's wind power-hydrogen production for fossil fuel hydrogen production, *J. Clean. Prod.* 422 (2023) 138410.
[11] J.X. Zhang, Z.H. Wang, Y. He, M.Y. Li, X.D. Wang, B. Wang, Y.Q. Zhu, K.F. Cen, Comparison of onshore/offshore wind power hydrogen production through water electrolysis by life cycle assessment, *Sustain. Energy Technol. Assessments* 60 (2023) 103515.
[12] H. Shin, D. Jang, S. Lee, H.S. Cho, K.H. Kim, S. Kang, Techno-economic evaluation of green hydrogen production with low-temperature water electrolysis technologies directly coupled with renewable power sources, *Energy Convers. Manag.* 286 (2023) 117083.
[13] H. Li, Research on control strategy for integrated photovoltaic water electrolysis-hydrogen fuel cell system, *Electr. Eng.* (18) (2023) 49–53.
[14] Y.L. Han, K.N. Shi, Y. Qian, S.Y. Yang, Design and operational optimization of a methanol-integrated wind-solar power generation system, *J. Environ. Chem. Eng.* 11 (3) (2023) 109992.
[15] A. Ibáñez-Rioja, L. Järvinen, P. Puranen, A. Kosonen, V. Ruuskanen, K. Hynynen, J. Ahola, P. Kauranen, Off-grid solar PV–wind power–battery–water electrolyzer plant: simultaneous optimization of component capacities and system control, *Appl. Energy* 345 (2023) 121277.
[16] X.F. Shi, Y. Qian, S.Y. Yang, Fluctuation analysis of a complementary wind–solar energy system and integration for large scale hydrogen production, *ACS Sustainable Chem. Eng.* 8 (18) (2020) 7097–7110.
[17] Y. Ren, K.Y. Jin, C.L. Gong, J.Y. Hu, D. Liu, X. Jing, K. Zhang, Modelling and capacity allocation optimization of a combined pumped storage/wind/photovoltaic/hydrogen production system based on the consumption of surplus wind and photovoltaics and reduction of hydrogen production cost, *Energy Convers. Manag.* 296 (2023) 117662.
[18] L. Phan-Van, V.N. Dinh, R. Felici, T.N. Duc, New models for feasibility assessment and electrolyser optimal sizing of hydrogen production from dedicated wind farms and solar photovoltaic farms, and case studies for Scotland and Vietnam, *Energy Convers. Manag.* 295 (2023) 117597.
[19] H.J. Yang, M. Zhou, Z.Y. Wu, M.Y. Zhang, S.W. Liu, Z. Guo, E.S. Du, Exploiting the operational flexibility of a concentrated solar power plant with hydrogen production, *Sol. Energy* 247 (2022) 158–170.
[20] Y.M. Zhang, Z. Wang, Z.Y. Du, Y. Li, M. Qian, J. van herle, L.G. Wang, Techno-economic analysis of solar hydrogen production *via* PV power/concentrated solar heat driven solid oxide electrolysis with electrical/thermal energy storage, *J. Energy Storage* 72 (2023) 107986.
[21] D.Q. Zhao, Z.P. Xia, M.T. Guo, Q.J. He, Q.D. Xu, X. Li, M. Ni, Capacity optimization and energy dispatch strategy of hybrid energy storage system based on proton exchange membrane electrolyzer cell, *Energy Convers. Manag.* 272 (2022) 116366.
[22] Z.L. Wang, H.Y. Zhu, D.D. Zhang, H.H. Goh, Y.X. Dong, T. Wu, Modelling of wind and photovoltaic power output considering dynamic spatio-temporal correlation, *Appl. Energy* 352 (2023) 121948.

[23] V. Khare, S. Nema, P. Baredar, Solar–wind hybrid renewable energy system: a review, *Renew. Sustain. Energy Rev.* 58 (2016) 23–33.
[24] K. Anoune, M. Bouya, A. Astito, A. Ben Abdellah, Sizing methods and optimization techniques for PV-wind based hybrid renewable energy system: a review, *Renew. Sustain. Energy Rev.* 93 (2018) 652–673.
[25] H. Ali Muhammad, M. Naseem, J. Kim, S. Kim, Y. Choi, Y.D. Lee, Solar hydrogen production: technoeconomic analysis of a concentrated solar-powered high-temperature electrolysis system, *Energy* 298 (2024) 131284.
[26] N. Zhang, Y.H. Yu, J.W. Wu, E.S. Du, S.M. Zhang, J.Y. Xiao, Optimal configuration of concentrating solar power generation in power system with high share of renewable energy resources, *Renew. Energy* 220 (2024) 119535.
[27] A. Khiareddine, C. Ben Salah, D. Rekioua, M.F. Mimouni, Sizing methodology for hybrid photovoltaic/wind/hydrogen/battery integrated to energy management strategy for pumping system, *Energy* 153 (2018) 743–762.
[28] A. Lewandowska-Bernat, U. Desideri, Opportunities of power-to-gas technology in different energy systems architectures, *Appl. Energy* 228 (2018) 57–67.
[29] G. Maggio, A. Nicita, G. Squadrito, How the hydrogen production from RES could change energy and fuel markets: a review of recent literature, *Int. J. Hydrogen Energy* 44 (23) (2019) 11371–11384.
[30] Y.X. Liu, L.Z. Yao, B. Zhao, J. Xu, S.Y. Liao, X.P. Pang, Low carbon economic scheduling of distribution network-microgrid group considering flexible group behavior, *Energy Reports* 48 (20) (2024) 59–68. (in Chinese)
[31] R. Chen, Z.H. Rao, S.M. Liao, Determination of key parameters for sizing the heliostat field and thermal energy storage in solar tower power plants, *Energy Convers. Manag.* 177 (2018) 385–394.
[32] D.H. Zhang, Y.Y. Yun, X.J. Wang, J.H. He, H.Y. Dong, Economic dispatch of integrated electricity-heat-gas energy system considering generalized energy storage and concentrating solar power plant, *Automation. of. Electric. Power. Systems* 45 (19) (2021) 33–42.
[33] S.M. Saba, M. Müller, M. Robinius, D. Stolten, The investment costs of electrolysis–A comparison of cost studies from the past 30 years, *Int. J. Hydrogen Energy* 43 (3) (2018) 1209–1223.
[34] Y. Xu, R. Du, J.M. Pei, The investment risk evaluation for onshore and offshore wind power based on system dynamics method, *Sustain. Energy Technol. Assessments* 58 (2023) 103328.
[35] A. Barbón, V. Carreira-Fontao, L. Bayón, C.A. Silva, Optimal design and cost analysis of single-axis tracking photovoltaic power plants, *Renew. Energy* 211 (2023) 626–646.
[36] Z. Abdin, K. Khalilpour, K. Catchpole, Projecting the levelized cost of large scale hydrogen storage for stationary applications, *Energy Convers. Manag.* 270 (2022) 116241.
[37] Y.Q. Yang, S. Bremner, C. Menictas, M. Kay, Battery energy storage system size determination in renewable energy systems: a review, *Renew. Sustain. Energy Rev.* 91 (2018) 109–125.
[38] M. Mubarrat, M.M. Mashfy, T. Farhan, M.M. Ehsan, Research advancement and potential prospects of thermal energy storage in concentrated solar power application, *Int. J. Thermofluids* 20 (2023) 100431.
[39] X.H. Xu, K. Vignarooban, B. Xu, K. Hsu, A.M. Kannan, Prospects and problems of concentrating solar power technologies for power generation in the desert regions, *Renew. Sustain. Energy Rev.* 53 (2016) 1106–1131.
[40] A.N. Yerudkar, D. Kumar, V.H. Dalvi, S.V. Panse, V.R. Gaval, J.B. Joshi, Economically feasible solutions in concentrating solar power technology specifically for heliostats–A review, *Renew. Sustain. Energy Rev.* 189 (2024) 113825.
[41] Y.D. Hu, R.R. Zhai, L.T. Liu, H. Yin, L.Z. Yang, Capacity optimization and performance analysis of wind power-photovoltaic-concentrating solar power generation system integrating different S-CO_2 Brayton cycle layouts, *J. Clean. Prod.* 433 (2023) 139342.
[42] Y.L. Xiao, C.Z. Zou, M.Q. Dong, H.T. Chi, Y.L. Yan, S.L. Jiang, Feasibility study: economic and technical analysis of optimal configuration and operation of a hybrid CSP/PV/wind power cogeneration system with energy storage, *Renew. Energy* 225 (2024) 120273.